

DEBRIS FLOW HAZARD MODELING WITH GIS AND REMOTE SENSING IN
SOUTHERN CALIFORNIA

By Erica Paige Byerley

A Thesis

Submitted in Partial Fulfillment
of the Requirements for the Degree of
Master of Science
in Applied Geospatial Sciences

Northern Arizona University

April 2021

Approved:

Mark Manone, M.A., Chair

Ruihong Huang, Ph.D.

Taylor Joyal, Ph.D.

ABSTRACT

DEBRIS FLOW HAZARD MODELING WITH GIS AND REMOTE SENSING IN
SOUTHERN CALIFORNIA

ERICA PAIGE BYERLEY

Debris flows are important processes for transporting sediment and large debris in mountain streams, but have proven deadly for residents of Southern California. Wildfire drastically increases the probability of debris flow occurrence because vegetation is burned off while the soil is baked, accelerating runoff and impeding infiltration. Large populations often reside downstream of mountain washes where these flows occur, putting them at risk. With larger, more destructive wildfires, and more extreme precipitation patterns, this risk is increasing. Case studies of debris flows following the Thomas, Holy, Woolsey, and Station fires offer lessons on how to better manage risk and respond to these dangers. Variables likely to contribute to debris flow occurrence within watersheds of the burn scars were analyzed with GIS and ordinary least squares regression modeling to determine whether debris flow hazard models relied upon by local governments were appropriate. Variables found to be statistically significant correlate strongly with those used by the USGS Western Preliminary Hazard Assessment Model, indicating its robustness in Southern California. However, reliability could be improved by including forecasted precipitation intensities for a storm by GIS analysts at the local level rather than utilizing model storm precipitation. Local government's ability to effectively manage risk depends on debris flow hazard modeling capabilities, communication with the public, and coordination of emergency response by various government agencies. By implementing better policy in these areas, human life and property can be better protected when debris flows inevitably occur in Southern California again.

Acknowledgments

I would like to express sincere appreciation to my committee chair, Professor Mark Manone, for his support and flexibility throughout the evolution of this thesis project. When I first came to his office, fresh off a Colorado River trip, I was tentative about how I should move forward with a life and career off the river. He encouraged me to pursue this master's program as well as wherever my interest in debris flows took me. When Covid-19 struck and opportunities for fieldwork disappeared, he was supportive of the remote approach I decided to take. When I struggled with burnout and feared not being able to graduate on time, he encouraged me to persevere. Without his guidance and support, my accomplishments here at Northern Arizona University would not have been possible.

I also owe deep gratitude to my committee members, Professors Ruihong Huang and Taylor Joyal. Professor Huang's mastery of the GIS and Python skills I needed to complete this project was an inspiration. Professor Joyal's class on Arid Land Geomorphology was foundational to my understanding of debris flows and opened my mind to new ways of thinking about familiar problems in the Southwest. Learning as much as I have from both of them has been a profound privilege.

I would also like to thank my roommate Lori Anderson for being so considerate of my needs as a graduate student during a very difficult time in my life, and to thank my friends and family for their love and encouragement despite my long periods of absence. As I wrap up this chapter of my journey, I am humbled to be surrounded by so many amazing individuals whose support has truly made this thesis possible.

Table of Contents

Title Page.....	i
Abstract.....	ii
Acknowledgments.....	iii
Table of Contents.....	iv – v
List of Figures.....	vi
Introduction.....	1 – 7
Objectives.....	5-7
Literature Review.....	8 – 43
Limitations of Western Views of Nature.....	8 – 10
Background on Debris Flow Modeling.....	10 – 13
Variables Influencing Debris Flow Occurrence.....	13 – 23
Regression Modeling.....	23 – 25
Case Studies.....	25 – 43
Thomas Fire.....	25 – 29
Holy Fire.....	30 – 33
Woolsey Fire.....	34 – 37
Station Fire.....	38 – 43
Data.....	43 – 45
Study Areas.....	43
Important Dates.....	44
Data File Names.....	44 – 45

Methods.....	45 – 58
Pre-Processing.....	45 – 46
Delineating Watersheds.....	46 – 48
Satellite Imagery.....	48 – 49
Remote Sensing Indices.....	49 – 50
Other Variables.....	50 – 51
List of Variables.....	52
Python Scripting.....	52 – 55
Debris Flow Identification.....	55 – 59
Comparing Variables in Regression.....	58
Results.....	58 – 63
Remote Sensing.....	58 – 60
Regression.....	64 – 68
Discussion.....	64 – 68
Conclusion.....	69
References.....	70 – 77
Appendices.....	78 – 89
Appendix I: Metadata for Downloaded Files.....	78 – 81
Appendix II: Python Codes.....	82 – 87
Appendix III: OLS Regression Tables.....	88 – 89

List of Figures

Figure 1. Debris flow imagery following the Thomas fire.....	25
Figure 2. Debris flow imagery following the Holy fire.....	30
Figure 3. Debris flow imagery following the Woolsey fire.....	34
Figure 4. The urban-wildland interface in Trancas Canyon, Malibu, CA.....	36
Figure 5. Debris flow imagery following the Station fire.....	38
Figure 6. Four study fires for debris flow hazard analysis.....	43
Figure 7. Watershed delineation steps for the Thomas fire.....	48
Figure 8. Debris flow deposits from San Ysidro Creek Watershed.....	56
Figure 9. Debris flow incision scars in San Ysidro Creek Watershed.....	57
Figure 10. Thomas fire remote sensing indices.....	59
Figure 11. Woolsey fire remote sensing indices.....	59
Figure 12. Holy fire remote sensing indices.....	60
Figure 13. Station fire remote sensing indices.....	60
Figure 14. OLS Results from the Thomas fire.....	61

Introduction

The risk posed by climate change has become a double-edged sword for residents of Southern California: wildfires are becoming larger and more destructive, and rainfall patterns much more extreme between dry and wet periods (Swain, Langenbrunner, Neelin, & Hall, 2018). These two factors together raise the likelihood for highly destructive debris flows to occur, in which high intensity rain leads to a mass wasting event. Debris flows can be conceptualized as a cross between a landslide and a flash flood, and can have enough sediment to enable them to partially float car-sized boulders or even cars. They are more likely to occur post-wildfire because of increased runoff (Neary, Koestner, & Youberg, n.d.). The waxy chaparral vegetation common in Southern California worsens this effect by leaving behind a hydrophobic residue on top of the soil when it is burned, impeding infiltration (Jordan, Turner, Nicol, & Boyer, 2006; Keller, 2019). Mountain ranges in Southern California are already prone to debris flows due to the strong orographic effect they induce on frontal storms coupled with a natural fire regime (City of Glendale, n.d.). As extreme weather events become more common in this region, with more wildfire and larger intensity storms, debris flows are likely to pose an even greater threat to human populations in the future.

Southern California has a long history of deadly debris flows. On Christmas Day of 2003, 14 people were killed by debris flows out of the San Gabriel Mountains in Los Angeles. The event that garnered the most media attention was the storm generating debris flows in Montecito, CA on January 9, 2018. An intense storm unleashed 0.59 inches of over 30 minutes in the burn scar of the Thomas fire, which was still actively burning at the time (Molina, 2019). Debris flows ripped down drainages near Santa Barbara early in the morning, taking 23 lives and destroying 130 homes (Mozingo, 2018). The USGS had released their preliminary hazard assessment model

results approximately a month earlier. Hydrologists had completed more advanced modeling two days prior to the debris flows, but evacuations remained voluntary despite a high degree of danger (Garcia, Hayden, Hopwood, Welsh, Yamamura, & Smith, 2018).

Less eventful debris flows occur more often throughout Southern California and can also offer lessons on appropriate hazard mitigation strategies. Debris flows following the Woolsey fire in the Santa Monica Mountains and the Station fire in the San Gabriel Mountains were less destructive than the fires themselves, but still required extensive cleanup and emergency response (CBS Los Angeles, 2018; Kean & Staley, 2011).

There are many variables that may lead to a debris flow within a watershed. The most important of them all is rainfall. While other conditions necessary to trigger debris flows may be present in a watershed for months or even years, rainfall intensity is the catalyst (Bisson et al., 2005; Staley et al., 2018). Recent wildfire also increases the probability of debris flows occurring because loss of vegetation tends to increase runoff. Wildfires can significantly increase flood peakflows by reducing interception, reducing infiltration by burning surface organic matter, and increasing overland flow (Neary, Gottfried, & Folliott, 2003). Chaparral vegetation, common in the mountains of Southern California, can create hydrophobic soil when its waxy leaves burn, further increasing runoff (Jordan et al., n.d.). Precipitation may be concurrent with wildfire, triggering debris flows before mitigation strategies can be implemented (Staley et al., 2018). Burn severity can be determined through satellite imagery analysis and is often represented in the form of a differenced normalized burn ratio (dNBR), but field-verified burn severity data is preferred because different vegetation types can produce dNBR values that are not reflective of the burn severity (Staley et al., 2018).

Logistic regression analyses of many variables in various environments have been instrumental in determining other significant factors causing debris flows. In Saudi Arabia, researchers found topographic position index, slope, distance to drainage line, and normalized differenced vegetation index (NDVI) to be the most important from an analysis of 10 different variables (Elkadiri et al., 2014). In a logistic regression analysis from debris flows in Southern California as well as the Western U.S., the most important variables were determined to be: the basin area with slopes greater than 30 degrees, basin area burned at moderate and high severity, and total storm rainfall (Gartner et al., 2007). Most significantly, these researchers found that a critical angle for the significant erosion of burned soils was approximately 30 degrees. For the debris flows in Montecito, CA, scientists determined that the normalized burn ratio, hypsometric integral, and short-duration rainfall data could be used to predict which watersheds would have debris flows with 95% accuracy (Cui, Cheng, & Chan, 2019). The hypsometric integral is a quantitative index representing the relationship between the horizontal section area and its elevation in a watershed (Cui et al., 2019). These studies indicate that debris flow risk can be largely determined through variables derived from remote sensing and GIS spatial analysis products of digital elevation models (DEMs).

Availability of data largely determines what type of model is appropriate to use, and this holds true for debris flow modeling as well. In the case of massive wildfires, the time or budget might not be available for data collection in the field. Without data on soil burn severity, infiltration rate, and gully and rill formation following fire, physical modeling becomes impossible. Furthermore, accurate maps for creating debris flow or flood extent should use DEMs with resolutions of 4m or better (Stolz & Huggel, 2008), which are often not available.

Therefore, physical modeling is not practical for large regions that have been burned. Empirical modeling is a better approach. Simple models constructed using analysis from remote sensing and DEMs with 30m resolution have proven very effective in determining which watersheds will experience debris flows over large regional areas (Cui et al., 2019). Determining sediment supply or how much sediment will be mobilized given a specific rain intensity is complicated. Physical models requiring extensive fieldwork and complicated algorithms attempting to model unpredictable debris flow volumes and extents may not be as important for risk management. However, if volume or debris flow extent is deemed important by local governments to assess evacuation recommendations, a predictive hazard model based on remote sensing variables could identify priority watersheds for more advanced fieldwork-based modeling. This could potentially save valuable labor resources by limiting fieldwork-collected data to watersheds that only present the greatest risk to downstream communities.

A regression analysis performed on historic Southern California wildfires that had debris flows would illuminate the variables that are most significant in causing them. Once these are determined, a simple predictive model for post-wildfire debris flows in Southern California can be constructed for various storm conditions. For it to be effective as a rapid-response model, it also needs to be easy to use and widely distributable. A toolkit for debris flow modeling can be added to any local government's ArcGIS Pro arsenal, which could potentially streamline post-fire debris flow modeling and hopefully make emergency response to these events more proactive. Scripts written in Python can be used directly with ArcGIS Pro software.

Even a hypothetical model that is 100% accurate will not be sufficient for mitigating risk to Southern California residents from debris flows. Human factors also play a significant role. Populations living in the urban-wildland interface must completely rely on engineered debris

basins, channelized washes, and maintenance of these structures to keep them safe during storms following wildfire. A wide array of governmental agencies fight the fire, assess the watershed post-fire, clean out debris basins, release models and maps, communicate with the public, and respond to emergencies during storm events. They need to be able to coordinate efficiently in order to mitigate risk properly. Furthermore, it is extremely important for the public to be educated regarding the dangers of flash floods and debris flows so that they will keep themselves safe. Educational materials must also be made available in Spanish for the large Hispanic population in the region. If these qualitative issues are not addressed when local governments are creating emergency management plans, loss of life and destruction of property will continue to be a significant problem during post-fire storm events.

Personal Objectives:

There are many different approaches for modeling debris flows, which may all be appropriate under different circumstances. A remote approach can be appropriate when there is little or no time between the fire and potentially destructive storm, when such large areas have been burned that fieldwork is impractical, or when terrain is too rugged or remote. Because the majority of my research took place during the year 2020, Covid-19 placed an additional barrier to in-person science. I chose a GIS and remote sensing-based approach to learn how these technologies could contribute to our understanding of debris flow hazard when other approaches are not possible. Furthermore, I wanted to use this time as an opportunity to develop computer skills learned throughout my M.S. Applied Geospatial Sciences program. The Python codes I wrote for analyzing variables within watersheds are a substantial portion of this body of work and will be useful in future watershed science I may participate in. Lastly, I wanted to learn how

these skills might be marketable to potential employers and fit in with existing strategies for mitigating debris flow hazard to residents of Southern California. For these reasons, it was important to consider debris flow hazard from both a scientific as well as policy perspective. A thorough understanding of policy through case studies of each fire included in the scientific analysis was necessary in order to provide context. Policy can inform how science should best be applied. Therefore, my research throughout this project will attempt to address two primary questions:

1. How can policy be shaped to mitigate debris flow risk to Southern California residents?
2. What scientific variables are most important for debris flow initiation in this region?

Research Objectives:

- 1) Conduct a literature review on scientific variables influencing debris flow initiation as well as qualitative factors that influenced hazard in each study fire.
- 2) Extract or obtain DEM models for selected areas to a resolution of 10m, and use these to develop watershed boundaries for use in the debris flow model.
- 3) Determine the variables most likely to cause debris flows that we can measure through remote sensing processes (NBR, NDVI, watershed slope, etc.). Obtain data from outside sources for other variables as necessary.
- 4) Use Python scripts to determine variable values for each watershed and write them into the watershed attribute table.
- 5) Identify debris flows for each watershed within a study fire burn area and note positive or negative identification in the watershed attribute table.

- 6) Apply ordinary least squares regression analysis to selected watersheds to determine which variables are statistically significant.
- 7) Report results and compare them with USGS Western Preliminary Hazard Assessment Model.
- 8) Make recommendations on how Southern California could better mitigate hazard from debris flows based on application of models and relevant policy.

The first chapter of this thesis consists of a literature review. This begins with a discussion of the difficulties in predicting or controlling water in the Southwest, which experiences highly variable precipitation. I then go into detail about debris flow modeling and variables that might influence debris flow initiation. Because it is important to consider policy and human geography for debris flows occurring in the highly developed urban-wildland interface of Southern California, case studies of the Thomas, Holy, Woolsey, and Station fires follow next.

The scientific analysis of these study fires consists of the majority of my research and the second chapter of this thesis. Sections follow standard scientific format. Codes written in Python utilizing tools available in ESRI GIS software were used to analyze debris flow variables at the watershed scale. These variables were compared using ordinary least squares regression, where presence or absence of a debris flow within a watershed was the dependent variable. Results of this analysis are compared with variables used by the USGS Western Preliminary Hazard Assessment Model. A discussion including policy recommendations, conclusion, references, and appendices conclude this thesis.

Literature Review

Limitations of Western Views of Nature:

Western civilization and the United States specifically have a long history of trying to control nature. Our society has become overcommitted to the idea that we can bend rivers to our will, and effects of this hubris have been disastrous. In the Southwest, engineers and scientists seem to cling to the idea that every drop of water can be predicted and accounted for. The Colorado River Compact was signed during an unusually wet year, but the Colorado River does not regularly experience its “average” flow. Instead, it oscillates between long periods of either wet or dry extremes (Swain et al., 2018). High variability is expected. Overconfidence in predicting flow into Lake Powell nearly led to the demise of Glen Canyon Dam. Similarly, debris flow control structures regularly fail in Southern California because engineers do not have enough information to be able to accurately take all variables leading to debris flows into account. Western society should respect the power of rivers, whether large or ephemeral, and allow room for unpredictable fluctuations.

Glen Canyon Dam in northern Arizona holds back Lake Powell and regulates the flow of the Colorado River through Grand Canyon. In 1983, it was nearly lost because engineers neglected to account for the effects of cavitation when designing the emergency spillways. Although the Bureau of Reclamation knew that cavitation would likely lead to damage if the spillways were ever used, they planned to manage Lake Powell so well that this would not become a significant problem (Powell, 2010). The spillways were connected to worksite diversion channels at a steep angle to save time and money. However, they did in fact need to be used when a May snowstorm followed by a heatwave sent a large influx of unexpected water into Lake Powell and threatened to overtop the dam. Erosion at the spillway joints due to

cavitation began eating backwards at the thick concrete plugs filling the old diversion channels, nearly causing an “uncontrolled release” of the entire contents of full-pool Lake Powell, which would have destroyed each successive dam on the Colorado River downstream of Glen Canyon Dam (Powell, 2010). Believing that storms and runoff could be predicted so well that the reservoir was filled to the brim nearly led to the demise of this dam.

The idea that the current drought in the Colorado River Basin can be entirely attributed to climate change is an extremely anthropocentric view and ignores thousands of years of history of exceptionally variable precipitation. The Colorado River Compact attempted to settle water disputes between southwestern states and is the basis for water law in this region. It was signed during the wettest year of the 1900s, which was the wettest century in the last 2000 years (Parker, 2010). Determining water allocations in a year of surplus has led to shortages in subsequent years. There is no denying that significant drought has also negatively impacted the Southwest in recent years. However, because the region has historically endured persistent drought, it is not scientific to claim the most recent one is purely due to climate change. While climate change is impacting precipitation regimes around the world and is likely to make the Southwest even drier and hotter, it was expected to return to a drier and hotter stage anyway based on its long historical climate patterns. Western society needs to acknowledge that it can't predict or control everything, even in a negative way. Instead, more respect and space should be given to nature's power and variability.

Similarly, attempts at controlling debris flows in Southern California are likely to fail because of the unpredictable nature of the Southwest's variable precipitation regime. “A debris basin that serves well in one year may not be adequate in another. [...] Designs are focused on the ‘ten-year flood,’ the ‘twenty-five-year flood,’ the ‘fifty-year flood,’ and maps depict the

‘once-in-a-hundred-years flood,’ but these terms rest on data of only a century and a half and represent educated guesses. Rain, moreover, is merely one factor. No wonder there are times when the basins fail” (McPhee, 1989). Engineers try to take expected precipitation into account, but sediment supply, burn severity, slope, etc. also contribute to debris flows. When scientists still don’t know the exact formula for debris flow volume, it is impossible to engineer structures to adequately contain them. Humans living on alluvial fans downstream of these mountain washes must trust the ability of engineers to control their environment more than they fear the debris flows that formed the land they live on.

It is from within a framework of humility that we need to approach the study of and response to debris flows within Southern California. Debris flows are like temporary rivers composed largely of mud and rocks. They are exceptionally difficult to model, especially when we can’t predict rain intensity and duration everywhere. Rivers need room to run, so predicting whether or not debris flows will occur rather than trying to predict and control every aspect of their flow seems like a better strategy for success. When it is not possible to know every house or road that will be destroyed during a storm, we should instead evacuate all homes and close all roads that *might* be affected. Debris flow control structures, if absolutely necessary, should be designed for the high end of known flows. Southern CA is especially vulnerable because it has left no room for rivers to run, for nature to be wild. It has relied entirely on control. So, wilderness regularly comes knocking down the door.

Background on Debris Flow Modeling:

There is increased demand for development of feasible methodologies for hazard assessment, especially for areas that have a limited availability of data (Bisson et al., 2005). Data

is limited in large areas that have been burned by wildfire because of difficulties associated with fieldwork in rugged terrain. Debris flows regularly occur in extremely steep mountains, making data collection difficult, expensive, and time consuming (Elkadiri et al., 2014). The fire may also still be burning in study areas of interest. Furthermore, storms may occur in areas recently burned before there is enough time to obtain detailed information sufficient for development of risk mitigation strategies. Recently burned areas may even generate convective storms over them, triggering debris flows before strategies can be implemented (Staley et al., 2018). This further underscores the need for a simple, quick model that doesn't rely on large amounts of high-resolution data.

Researchers in Sicily came up with a method for rapidly analyzing areas of potential debris flows. They used a 30m DEM (which is a low enough resolution to be publicly available everywhere) in their study with good results. They used the IFIRE index instead of NBR, and slope and hillslope curvature instead of hypsometric integral to quickly identify areas of potential hazard (Bisson et al., 2005). They recommend that this type of assessment be used to highlight areas in need of more detailed modeling, which is the same approach that is needed in Southern California.

Analysis of DEM grid spacing for determining potential hazard zone of debris flows in Switzerland found that grid resolution is crucial (Stolz & Huggel, 2008). DEMs with 4m and 1m resolution were effective in confining the debris flow in the model to the channel. This level of accuracy would be useful for a debris flow volume or extent model, and could determine how many homes lie in the path of potential debris flows. However, a goal of my research is simply to determine whether or not a watershed will have a debris flow, so this level of detail is

unnecessary for my project. Researchers found a 25m DEM to be sufficient for providing an approximate estimation of the potential hazard zone.

The USGS regularly releases post-wildfire debris flow hazard maps for significant fires in Southern California. This model is heavily relied on and distributed to the public. It consists of combined probability and volume models to create a map of total hazard for each watershed within the burn area. Variables used for the probability model are the average dNBR of the upslope area, the soil K factor, the proportion of upslope area in burned area reflectance class (BARC) Class 3 or 4 with gradients $\geq 23^\circ$, and the peak 15-minute rainfall accumulation (USGS, 2021). It is unusual that this model relies on two different variables involving burn severity.

Researchers found that early warning systems triggered by real-time data from monitoring stations in burn areas are not suitable for warning downstream communities of impending debris flows (Kean, Staley, & Cannon, 2011). Realistically, people need lead times of hours to properly prepare for evacuation from their homes. Improvement in predictions of short-duration high-intensity rainfall would be helpful so that experts can have more certainty whether watersheds would reach the threshold for debris flow initiation. Local GIS experts are needed to model debris flow hazard from the most up-to-date forecasts available.

It is impossible to talk about mitigating future fire risk without mentioning climate change. Increasing temperature is likely to both lengthen the duration of the fire season in Southern California as well as increase the total area burned (McKenzie et al., 2004). As California begins to see more destructive fires, its risk of subsequent debris flows will also increase. Massive storms are not necessary to trigger a debris flow since the soil stability due to fire and the underlying geology are more important factors. If an area has been severely burned,

the potential for flooding and natural disasters will significantly increase even with average rainfall (Kean & Staley, 2011).

Population growth in this region is expected to continue, so potential damage to life and property is likely to continue to increase as well (Robichaud et al., 2009). Greater populations living in fire-prone country also increases the risk of fire, as there are more people to potentially start them. Since managing human activity and prescribing controlled burns in the chaparral are not great options, it seems as though little can be done to mitigate fire risk. However, direct seeding of recently burned areas can profoundly increase vegetation return rates (Robichaud et al., 2009). This is a low-cost option that could prove beneficial to residents of Southern California who will be especially vulnerable to debris flows over the next few years. Improving GIS modeling capabilities, overhauling warning systems and debris flow education, and ensuring efficient communication between responding agencies are likely to have the most benefit.

Variables Influencing Debris Flow Occurrence:

1. Hypsometric Integral:

The hypsometric integral (HI) is one of the variables to be used in the logistic regression analysis. It is a quantitative index representing landform erosion stage and evolution process. It reflects the horizontal section area and its elevation in a watershed, serving as a proxy for watershed shape. In very simple terms, steep watersheds are much more likely to experience debris flows than watersheds with gentle slopes (Bisson et al., 2005; Elkadiri et al., 2014; Jordan et al., 2006). While there are different methods for calculating the HI value, the elevation-relief

ratio proposed by Pike and Wilson (Pike & Wilson, 1971) for estimating HI is both simple and efficient. It can be defined as:

$$HI \approx \frac{H_{ave} - H_{min}}{H_{max} - H_{min}}$$

where H_{ave} is the average elevation value of a watershed, H_{min} is the minimum elevation value of a watershed, and H_{max} is the maximum elevation value of a watershed. This is the method used by Cui, Cheng, and Chan in 2018, so this will be the way I estimate HI as well.

Another study for rapid assessment of fire-related debris flows in the Mediterranean climate of Sicily found that the most important parameters for triggering shallow landslides that become debris flows are slope and hillslope curvature, where concave hillslopes are most prone to failure (Bisson et al., 2005). The hypsometric integral is a single value that represents these two parameters.

2. *Burn Severity:*

Normalized Burn Ratio (NBR) images are commonly used for analyzing the effect of fire on an area. They are created with remote sensing using the bands capturing near infrared (NIR) and short wave infrared light (SWIR) in the electromagnetic spectrum (Bisson et al., 2005). Normalized Burn Ratio (NBR) for each wildfire will be calculated using images captured immediately before and after each burn, and is defined as:

$$\Delta NBR = NBR_b - NBR_p$$

where NBR_b is the NBR calculated before the burn and NBR_p is the NBR calculated immediately after the burn.

Field-verified burn severity data is also regularly used in debris flow modeling. The USGS relies on BARC classification for the debris flow likelihood component of its post-fire

debris flow hazard model (USGS, 2021). BARC classification is determined by the Burned Area Emergency Response (BAER) team, which “is made up of trained specialists in soils, hydrology, geology, botany, recreation, wildlife, engineering, and archaeology who rapidly evaluate burned areas in order evaluate the effects to watersheds, identify values at risk, and to protect life, property, and critical natural and cultural resources” (Nicita & Halverson, 2018). BAER teams analyze the soil burn severity from in the field, creating more reliable maps than can be determined through remote sensing alone. If this type of data is available, it is preferred to remotely sensed burn severity data because more accurate data will increase the certainty of debris flow hazard predictions.

3. *Slope*

Slope is an important variable for debris flow studies. High slopes tend to increase the probability of debris flow occurrence for several reasons. They increase precipitation runoff velocity, which lends the water more power to cause erosion. Sediment saturated by precipitation often fails on steep slopes because of entrainment of air and water, loss of independent motion of the constituent particles, increased hydrostatic pressure, and decreased shear strength of the sediment (Blair & Associates, 1999). This leads to debris flow initiation.

Slope is a common variable to include in debris flow studies. Sometimes slope is restricted to angles greater than 23 or 30 degrees when included as a study variable because of how important steep slopes are to debris flow initiation (Gartner, Cannon, Santi, & Dewolfe, 2008). In their logistic regression study of debris flows in Saudi Arabia, researchers expected increasing slope angle to be correlated with increasing debris-flow occurrences up to the point where the slope is too steep for soil layer development and debris accumulation (Elkadiri et al.,

2014). Without adequate sediment supply, flash floods are more likely than debris flows. The Jazan province in Saudi Arabia experiences 550 mm/year of rainfall from tropical air masses and the orographic effect induced by very steep mountains (Elkadiri et al., 2014). This environment is similar to the San Gabriel Mountains in Los Angeles, which also are extremely steep with intense structural deformation in the form of folds, faults, and fractures, and receive 440 mm/year in precipitation (Weatherbase, 2021). Vegetation loss due to fire increases the effect of slope on erosion because woody material and below-ground root structures cannot hold the soil in place (Miller, Billmire, Elliot, Endsley, & Robichaud, 2015). This explains why wildfire, though not a prerequisite, is often associated with debris flows in the burn scar in subsequent years.

4. Normalized Differenced Vegetation Index (NDVI)

Vegetation is an extremely important variable leading to debris flows. First of all, it increases surface roughness. Greater surface roughness slows both water and wind down, which increases infiltration and decreases erosion. Vegetation significantly increases infiltration because interception can reduce surface sealing that is common in dryland environments (Joyal, 2020). It also increases the hydraulic conductivity of the soil through lateral root distribution, further increasing infiltration (Chen, Sela, Svoray, & Assouline, 2013). Common vegetation types in Southern California are wetlands, riparian habitats, woodlands, coastal sage scrub, and four types of chaparral: chamise, Ceanothus, mixed, and redshanks (Ustin & Roberts, 1996).

Chaparral vegetation in particular is regionally important in the wildfire-debris flow cycle. It is adapted for fire, with a tendency to be very dry and catch fire easily. Some species will only germinate after a fire (Keeley, 1987). “The older chaparral becomes, the hotter it burns.

In its first ten years of new growth, it is all but incombustible. After twenty years, its renewed flammability curves sharply upward. It burns, usually, before it is forty years old. The hotter the fire, the more likely a debris flow—and the greater the volume when it comes” (McPhee, 1989). In combination with fall Santa Ana winds that bring hot, dry air downslope, chaparral fires quickly burn out of control. Fire suppression in this environment only leads to a buildup of dry, waxy leaves under chaparral plants, which causes larger and hotter fires when the area eventually does burn. It naturally burns about every 30 years.

Loss of vegetation following wildfire causes several important hydrologic changes: burning the organic litter layer can produce hydrophobic soils; without the litter layer, water storage capacity is decreased and the soil is not protected from erosion due to raindrop energy; the forest has no interception capacity; and less vegetation leads to less evapotranspiration and increased snow accumulation (Jordan et al., 2006; Neary, Gottfried, & Folliott, 2003). Effects can last for months and even years following the fire event (Bisson et al., 2005). The waxy and oily chemicals in chaparral vegetation are especially prone to creating hydrophobic soil when burnt, reducing infiltration and increasing runoff even more than other vegetation types (Keller, 2019). This drastically increases runoff from storms in burned watersheds. In a watershed in the California chaparral, researchers observed a peakflow increase of 870-fold following a wildfire (Neary, Gottfried, & Folliott, 2003). Greater stream power increases erosion potential and increases the probability of debris flow occurrence.

Remote sensing can measure the amount of living vegetation in a landscape through an index value called the Normalized Differenced Vegetation Index (NDVI). This is done by comparing values reflected by the landscape of near-infrared wavelengths (NIR) and red

wavelengths, which is a formula sensitive to concentrations of chlorophyll at the surface (Elkadiri et al., 2014). The formula for this index value is:

$$NDVI = (NIR - Red) / (NIR + Red)$$

Healthy vegetation will reflect low amounts of red light but high amounts of NIR light (Roy et al., 2016). Because of vegetation's strong influence over watershed response to storm events, NDVI is an important variable to analyze to predict debris flow hazard. It was found to have a strong correlation with debris flows in Saudi Arabia (Elkadiri et al., 2014).

5. *K Factor (Soil Erodibility Factor)*

Soil erodibility is another important factor to consider. The K factor of a soil represents the susceptibility of the soil to erosion and the rate of runoff (NRCS-USDA State Office of Michigan, 2002). Soils high in silt are most easily eroded and will have high K factors (>0.4). Soils that have low runoff or are not easily detachable have low K factors, like sandy or clay-heavy soils. Organic matter content lowers the K factor because it increases infiltration and reduces the soil's susceptibility to detachment. The K_f factor considers only the finest soil fragments <2.00mm, while the K_w factor considers the whole soil. The K factor is often used in the Revised Universal Soil Loss Equation (RUSLE), which contributes to research on soil erosion and its effect on agricultural productivity (NRCS-USDA State Office of Michigan, 2002). Its importance in debris flow processes is reflected by being one of the few variables used by the USGS Western Preliminary Hazard Assessment Model (USGS, 2021).

6. *Percent Clay*

Alluvial fans can provide a rich record of paleoenvironmental conditions due to their ability to trap the majority of sediment from a mountain catchment (Harvey, Mather, & Stokes, 2005). Climate change may induce incision on alluvial fans due to base-level change of seas, lakes, or axial rivers, as seen in the stratigraphy of Quaternary alluvial fans (Harvey et al., 2005). Catchment characteristics such as drainage basin area, relief, and geology are controlling factors on the supply of water and sediment to the fan and the resulting dominant process it undergoes (Blair & Associates, 1999; Harvey et al., 2005). The process responsible for the formation of an alluvial fan leads to its morphology and stratigraphy. For example, in Death Valley, CA, underlying geology was found to be the primary controlling factor determining whether alluvial fans with otherwise similar characteristics were subject to debris flows or sheetfloods as their dominant sedimentary process. The low permeability and unsorted nature of clay, mud, and boulders yielded on the Warm Spring fan led to debris flows, while the high permeability of sediment from weathered andesite and granite on the Anvil Spring fan led to dominance of sheetflood processes (Blair & Associates, 1999). While clay is more resistant to detachment and less likely to erode than siltier soils, under high rain intensities, its low permeability can cause increased runoff and ultimately higher stream power (NRCS-USDA State Office of Michigan, 2002). This may lead to a dominance of debris flow processes in watersheds throughout the mountains of Southern California. Percent clay content of the soil is therefore an important variable to consider for causing debris flows.

7. *Remotely Sensed Soil Indices*

Soil characteristics are very important for debris flow initiation. Soils may develop structural seals following wildfire, greatly impeding infiltration (Guilinger, Gray, Barth, & Fong, 2020). Additionally, dry ravel often primes a watershed for debris flows. Dry ravel is when soil, ash, and other debris slides downslope due to gravity, and is an especially important erosional process in very steep environments. It can lead to an immense buildup of sediment in canyon washes and increases exponentially (as much as 60x) following wildfire (McPhee, 1989). LiDAR would likely be the best way to remotely sense dry ravel accumulation in canyons, but this type of data is not currently easily accessible. Remotely sensed satellite data, however, is free and readily available.

Development of soil indices from satellite imagery can be challenging due to soil's similar spectral signature to water or shadows when moist, and to rocks or urban surfaces when dry (Deng, Wu, Li, & Chen, 2015). Many different soil indices exist for various purposes, but indices for determining bare or bright soil could be useful for predicting debris flow probabilities.

The Normalized Difference Soil Index (NDSI) is efficient at characterizing brightness of the soil (Sensing, Nordal, & Lindsay, 2017). This index is calculated with the following equation:

$$\text{NDSI} = \frac{\text{GREEN} - \text{BLUE}}{\text{GREEN} + \text{BLUE}}$$

Severely burned areas are much darker than unburned areas and could possibly represent areas with more hydrophobic soil, which are highly associated with debris flows. The Bare Soil

Index (BSI) might also be useful for debris flow predictive models because it is designed to identify areas of bare soil and fallow land. Bare soil has higher rates of runoff than vegetated areas, so is more likely to experience a debris flow. This index can be represented by the following equation:

$$BSI = \frac{(SWIR + R) - (NIR + B)}{(SWIR + R) + (NIR + B)}$$

Short Duration Heavy Rainfall

Rainfall intensity is also among the most important variables leading to post-wildfire debris flows. While other conditions necessary to trigger debris flows may be present in a watershed for months or even years, rainfall intensity is the catalyst (Bisson et al., 2005; Staley et al., 2018). NOAA weather station data is available for free public download. However, detailed precipitation records are not available for download after 2014. This lack of data availability is a substantial hindrance to the ability to conduct climate-related science. Since weather stations are point feature classes and rainfall intensities across entire watersheds would need to be determined, some method of interpolation would need to be used in order to rasterize this information. Stations might not be placed closely enough together for accurate interpolation regardless. Storm events often have extreme local variation in precipitation, and since rainfall is often the triggering factor causing debris flows, it is important to get the most accurate data possible for this input to the model flows (Montgomery, Schmidt, Dietrich, & McKean, 2009; Moody, Shakesby, Robichaud, Cannon, & Martin, 2013; Staley et al., 2018.).

Although exclusion of explanatory variables in modeling can lead to unreliable results, researchers have forgone precipitation intensity data in their logistic regression debris flow

model when it did not exist (Elkadiri et al., 2014). It has been found to be an extremely important variable in numerous other studies (Gartner et al., 2008; Guilinger et al., 2020; Moody et al., 2013).

Different rainfall intensities and durations will lead to different environmental responses from watersheds. Landslides are triggered by longer duration storms because increased soil saturation causes slope failure due to decreased shear strength of the soil (Montgomery & Dietrich, 1994). Debris flows differ because they are runoff-generated and can travel kilometers onto alluvial fans when “exceptionally intense rainfall occurs over steep, severely burned watersheds” (Guilinger et al., 2020).

Tall mountains tend to receive greater rainfall due to an orographic effect (City of Glendale, n.d.). Recently burned areas may also generate convective storms over them, triggering debris flows before mitigation strategies can be implemented (Staley et al., 2018). The San Gabriel Mountains experience exceptionally intense rainfall during winter storms because of their pronounced height and proximity to the Pacific Ocean. “Some of the most concentrated rainfall in the history of the United States has occurred in the San Gabriel Mountains. [...] In January, 1969, for example, more rain than New York City sees in a year fell in the San Gabriels in nine days” (McPhee, 1989). Their combination of intense wildfire, exceptionally steep slopes, and intense rainfall create the perfect setting for destructive debris flows to occur.

Attempts at controlling debris flows in Southern California are likely to fail because of the unpredictable nature of the Southwest’s variable precipitation regime. “A debris basin that serves well in one year may not be adequate in another. [...] Designs are focused on the ‘ten-year flood,’ the ‘twenty-five-year flood,’ the ‘fifty-year flood,’ and maps depict the ‘once-in-a-hundred-years flood,’ but these terms rest on data of only a century and a half and represent

educated guesses. Rain, moreover, is merely one factor. No wonder there are times when the basins fail” (McPhee, 1989). Engineers try to take expected precipitation into account, but sediment supply, burn severity, slope, etc. also contribute to debris flows. When scientists still don’t know the exact formula for debris flow volume, it is impossible to engineer structures to adequately contain them. Humans living on alluvial fans downstream of these mountain washes must trust the ability of engineers to control their environment more than they fear the debris flows that formed the land they live on.

Regression Modeling

The purpose of logistic regression modeling is to determine the variables that best predict a specific outcome (Elkadiri et al., 2014). The dependent variable is categorical and can only have values of either 1 or 0 (Cui et al., 2019). Usually just a few variables will make the model very accurate and subsequent variables added will not make the model significantly more accurate in its predictions. This could be because variables are redundant or have reduced influence on the outcome of the dependent variable. Variables are added one at a time until the best model fit is determined. In a study conducted in the Red Sea Hills of Saudi Arabia, researchers used a logistic regression model to determine the most important variables for predicting debris flows. Ten variables were considered that could influence debris flows: slope angle, slope aspect, normalized difference vegetation index, topographic position index, stream power index, elevation, flow accumulation, distance to drainage line, soil weathering index, and topographic wetness index. They found topographic position index, slope, distance to drainage line, and normalized differenced vegetation index (NDVI) to be the most important (Elkadiri et

al., 2014). Rainfall can trigger debris flows at different intensities depending on the relative values of the other variables.

This method is reliable, cost-effective, and applicable to regions lacking high-resolution data. These findings are fairly similar to the variables used by Cui et al. (2018) in Montecito. Hypsometric integral reflects landform erosion stage and evolution process, and its elevation-relief ratio is somewhat of a substitute for topographic position index, slope, and distance to drainage line used by Elkadiri et al. (2014). NBR is somewhat correlated with NDVI in the sense that it provides a numerical value representing the state of the ground cover. Areas that have been more severely burned will have significantly less vegetation. Similarity of variables considered important for triggering debris flows in extremely different regions of the world are encouraging.

Ordinary least squares (OLS) is a regression technique that is considered the starting point for all spatial regression analyses (ArcGIS Pro 2.7, 2021). It generates a single regression equation indicating the relative strength of individual variables in determining the value of the dependent variable. In the case of debris flow hazard modeling, a debris flow in a watershed (the dependent variable) can be represented as '1' and lack of a debris flow '0'. Explanatory variables are weighted with coefficients that can be positive or negative, indicating how they affect a debris flow outcome. Multiple and Adjusted R-squared values measure the equation's ability to explain the variability in the dependent variable and therefore are values representing the model's performance. The T-test determine which variables are statistically significant, and the Koenker test determines whether probability values or robust probability values should be analyzed. VIF values measure redundancy among explanatory variables, and indicate some variables should be removed from the model when those values are too high. If residuals are

found to be spatially autocorrelated, an explanatory variable may be missing from the model, known as misspecification. Results from a model in this case would not be trustworthy.

Case Studies

A. *Montecito, CA: Thomas Fire Debris Flows*



Figure 1. Debris flow imagery following the Thomas fire.

The Thomas fire burned throughout Santa Barbara County December 2017- January 2018. This fire is what truly set the stage for the Montecito debris flow because intense precipitation following a major wildfire is likely to lead to disaster (Keller, 2019). This is exactly

what happened to residents of Montecito: they were devastated by the Thomas fire and then hit with an intense storm with no time for vegetation to recover in between.

In the middle of the night on January 9, 2018, the skies opened up over Montecito, CA and released a torrent of 0.59 inches of rain in a half an hour. This water ripped apart hillsides recently burned by wildfire and sent a deluge of mud downstream which obliterated and collected anything in its path, including vehicles and parts of homes. To make matters worse, the storm hit at approximately 3:30 in the morning (Molina, 2019), so victims and responders were trying to navigate through this entirely new, moving landscape in darkness. In total, 100 single-family homes were destroyed in this debris flow and 300 others were damaged (Molina, 2019). The 101 freeway was so terribly flooded that it had to be closed for almost 2 weeks, which cut off this beachside community, as well as the surrounding city of Santa Barbara, from the rest of Southern California. The greatest damage, however, was the tremendous loss of human life caused by this event. 23 people died as a result of the Montecito debris flows, 2 of which are still missing.

The UCSB Debris Flow Research Team has delved into the reasons behind the Montecito debris flow of January 9, 2018 specifically. Santa Barbara County has also released a Recovery Plan and an 'After-Action Report and Improvement Plan' to examine what went wrong during the initial event as well as what should be done to lessen future risk. Both these plans focus on human infrastructure and evacuation protocol rather than restoring the creeks or watersheds themselves.

The county was aware that debris flow hazard was high, and they expended effort clearing debris basins up until the flow occurred (County of Santa Barbara Office of Emergency Management, 2018), although this effort was nowhere near enough. Basins quickly filled during

the storm and the flows continued their path of destruction towards the sea. An incredible cleanup effort with volunteer assistance was implemented in the county after the debris flows. 100,000 tons of debris was moved and 12,000 pounds of hazardous materials had to be cleaned up (County of Santa Barbara Office of Emergency Management, 2018). Lots of infrastructure needed repair. During the disaster, 200 culverts, 20 bridges, and 50 miles of road were impacted. Several natural gas pipelines exploded during the debris flow and caused structural fires (County of Santa Barbara Office of Emergency Management, 2018). These needed to be repaired and the county has also recognized the need to introduce new infrastructure to assist residents during emergencies.

A significant portion of the remaining effort went into management of impacted people. Not all groups were affected equally. Researchers found that renters, residents of voluntary evacuation areas, and informal workers were the most at risk (Goto, Gray, Keller, & Clarke, 2021). A significant addition to their vulnerability was a failure by local authorities to properly educate residents regarding the dangers of debris flows. Marginalized communities tend to be most affected by natural disasters. When they survive, they often lose their livelihoods and become even more vulnerable (Wisner & Luce, 1993). The consistent burdening of certain groups of people by natural disasters is a tragic outcome, especially in a place with as high a cost of living as Southern California. Protocols should ensure that all groups are equally protected.

Massive debris flows are a natural part of the ecosystem and cannot be completely controlled. Attempting to restore Montecito to the way it was before the disaster or re-building in the Montecito Creek corridor, which was hit the hardest is not prudent (Molina, 2019). “The most effective response to the flash flood and debris flow hazard is to just say no to development along potential flow paths. [...] damage in the lower parts of the debris flow fans and alluvial

fans will remain a hazard as channel position is uncertain and may change from flow to flow as the fan morphology develops” (Keller, 2019). With the vegetation cleared by fire in the headlands and by the debris flow itself lower in the watershed, the whole channel is unstable. It needs time for vegetation to regrow and for the channel to establish its new normal. This holds true particularly for areas on or downstream of vulnerable geology, like shale. However, the town of Montecito considers rebuilding an essential step towards recovery. Society should recognize that it cannot control the environment completely. Instead, it should respect the potential power of debris flows by not building directly in their paths, and by improving on evacuation protocol and emergency response capabilities.

Communication regarding evacuation mandates could also be significantly improved. Traditional communication methods are often impaired during emergencies, sometimes interrupting television, internet, and cell phone service. Radio is a crucial tool during these times, and efforts have been made with local and regional radio stations to further support information dissemination, including broadcasting messages in Spanish (County of Santa Barbara Office of Emergency Management, 2018). They are considering exploring a siren warning system (County of Santa Barbara, 2018). Keeping as many lines of communication open as possible during emergencies is critical for keeping people updated so that they can respond appropriately.

Public education is something else that can be done that has the potential to greatly reduce loss of human life in future debris flows. Many people did not respond to the order to evacuate, and many residents of Montecito had never even heard of a debris flow before January 9, 2018 (Keller, 2019). Some people do not think the term “debris flow” adequately conveys their destructive potential, so many may not have taken the order seriously enough. If the public

is better educated about the potential danger of debris flows, especially following major fires, they will likely be more responsive to future calls to action and evacuation.

Santa Barbara County recognized the need for better dissemination of GIS maps with information capturing evacuation areas (County of Santa Barbara, 2018; County of Santa Barbara Office of Emergency Management, 2018), including updating the risk map as vegetation continues to grow in the burn scars of the Thomas Fire. These areas will continue to be a threat for future debris flows for the next few years (County of Santa Barbara, 2018), so monitoring natural response and vegetation regrowth is important. Reseeding burnt areas could promote vegetation growth and reduce the risk of damaging flows in the years following fire, but is likely one of very few practical solutions for manipulating the environment in response to this risk. Maps made with GIS should also show homes in the mandatory evacuation area parcel by parcel for them to be more accessible to residents. It would be helpful to be able to address different potential impacts of rainfall intensity vs. rainfall duration, such as the likelihood for flooding, landslides, or debris flows. The county has already hired more GIS personnel to help meet this need.

The debris flow of January 9, 2018 that ran through Montecito, CA was unbelievably destructive and traumatizing for its residents, but there is a lot that can be learned from this event. Loss of human life can be reduced by adjusting our response to these disasters, even when city planners insist on building in risky floodplains. Communication regarding evacuations can be improved by regularly updating maps and increasing their accessibility, relying on radio more heavily when power is out, and by improving public awareness of the danger of debris flows so they will be more likely to follow evacuation orders.

B. Temescal Valley, CA: Holy Fire Debris Flows

Debris flows from the Santa Ana Mountains
November 29, 2018
Temescal Valley, CA

Mud and debris from Horsethief Canyon is displayed on the right. Trabuco Creek experienced a significant debris flow that destroyed a bridge. Images below show debris on the bridge and cleanup efforts following the storm.



Figure 2. Debris flow imagery following the Holy fire.

The Holy Fire burned in Orange County in 2018. It was ignited by arson in Trabuco Canyon and burned approximately 9,400 acres of very steep chaparral-dominated terrain of the Santa Ana Mountains (Guilinger et al., 2020). Two major storms impacted the burn area: an atmospheric river on November 29, 2018 that produced peak I15 rain intensity of 14.4 mm/hr, and a cold front system on December 6, 2018 with a much greater peak I15 of 25.6 mm/hr (Guilinger et al., 2020). “Warning thresholds for debris flow initiation issued by the National Weather Service was 21 mm/hr, and the USGS Debris Flow Hazard Model indicated a 60-80%

probability of debris flows at 24 mm/hr” (Guilinger et al., 2020). The frontal storm on December 6, 2018 also caused debris flows in the Woolsey fire burn area. Although successive winter storms produced even greater rain intensities, these first two storm events are what led to debris flows in the Holy Fire burn area.

Researchers studying how postfire sediment sources and erosional processes change over multiple storm cycles found that sediment supplies are depleted more rapidly in the channel than on hillslopes, likely reducing sediment flux over time (Guilinger et al., 2020). Ash and fine material erode off steep mountain slopes even without rainfall, which is known as dry ravel. Dry ravel from fires often causes an exponential buildup of sediment in the channel, so the first storms in the wet season that move this sediment are what cause debris flows (McPhee, 1989). This explains why although rain intensity is the catalyst, even greater rain intensities will not always cause debris flows in the same canyons at later dates. Wildfire creates conditions in canyons like these prime for debris flows. The first storms of the season determine whether or not they occur and how destructive they will be.

Trabuco Creek Bridge was shut down due to debris flows out of Holy Jim Canyon (CBS Los Angeles, 2018). Road markings were not set out to indicate that the bridge was closed, causing anger among residents attempting to drive that way. Excessive traffic due to road closures and lack of communication is the opposite of an effective hazard mitigation strategy. As few people as possible should be in the vicinity of natural disasters in order to keep unimpacted roads clear for emergency responders. Reactionary rather than preemptive road closures are a significant part of this inefficiency. GIS can easily be used to determine bridges and roads that will be impacted in the event of a debris flow, as well as to find the fastest alternate paths. These analyses could be run before the storm if prioritized by local government.

Letitia Juarez of the local ABC News interviewed the mayor of Lake Elsinore, Natasha Johnson, regarding which neighborhoods would potentially be impacted by hillside debris flows. Some residents had been hit by mudslides and debris flows less than two weeks prior during the November 29, 2018 debris flows, so many had concerns despite evacuations being downgraded from mandatory to voluntary December 7. “We just don’t know the stability of our hills anymore,” Johnson said. “The fire did its devastation and as much as we can prepare for large sums of debris flow, the hills behind us that are not a concern could become a concern very quickly. So that is what takes place when we look at mandatory evacuations” (Juarez et al., 2018). During the rainy season, it is not uncommon for multiple storms to land in a few weeks. Rapid threat assessment tools are necessary to re-evaluate the conditions of burn areas for each successive storm. If fieldwork is not possible between storms, drones could be flown over the burn area to collect remote sensing data to determine how conditions and associated debris flow risk has changed. With so many lives and millions of dollars of property at risk, utilizing available technology provided by GIS specialists should be a priority.

Considerable effort was put in by many organizations to protect residents of Lake Elsinore from the danger of debris flows. Residential zones were classified for mandatory evacuation, voluntary, and at-risk (CBS Los Angeles, 2018). Sheriffs also went door to door to encourage people to evacuate. Following the Holy Fire, a “Watershed Emergency Response Team” (WERT) assembled with representation from geologists, civil engineers, hydrologists, foresters, and GIS specialists (Whiting, 2018). They issued a report highlighting infrastructure recommendations and survival tips. The Riverside County Flood Control and Water Conservation District was also active in managing debris retention basins both before and after the debris flows. “From September 2018 through April 2019, the estimated amount of total

nitrogen and total phosphorus removed from the Leach Canyon Dam and McVicker Debris Basin facilities was 7,527 tons and 120 tons, respectively” (Alta Environmental, 2019). These basins protect residents living along the wildland-urban interface by trapping sediment and debris, but can quickly fill up during storms, putting residents in danger when they overflow.

Coordination among different management agencies and areas of expertise is crucial for effective hazard mitigation. In the case of debris flows in the Lake Elsinore area following the Holy Fire, many different agencies responded to the debris flows: USGS, WERT, Riverside County Flood Control and Water Conservation District, the Fire Department, the mayor of Lake Elsinore, and local sheriffs. Better communication with the public regarding road closures would have drastically improved traffic flow and kept the public away from dangerous areas. Active GIS management and coordination with responders in the field could help to accomplish this risk management strategy.

C. Malibu, CA: Woolsey Fire Debris Flows

Debris flows and mudslides from the Santa Monica Mountains
January 5, 2019 and December 6, 2018
Malibu, CA

The Pacific Coast Highway was impacted by debris flows and mudslides the most (right and bottom left). Ocean-facing watersheds in the Santa Monica Mountains all drain in the ocean and cross the PCH. This section of highway can be closed for days following significant storm events before mud is cleaned out. A landslide scarp from debris flow producing storms threatens a Malibu home on the bottom right.



Figure 3. Debris flow imagery following the Woolsey fire.

The Woolsey Fire was the most destructive fire in Ventura and Los Angeles County history, killing 3 and destroying over 1,600 homes, including the mayor of Malibu's (Cosgrove, 2019). Questions have been raised regarding resource appropriation and evacuation policies. The Woolsey Fire was accidentally ignited by Southern California Edison, who will pay \$2.2 billion to settle insurance claims (Associated Press, 2021). However, limited resources were available to fight this fire because the Ventura County Fire Department was already battling the Hill Fire, and raging Santa Ana winds kept water-dropping aircraft grounded (Cosgrove, 2019). The company

was also found liable for the Thomas Fire and forced to settle for its extensive damage and following debris flows. Electric utility companies sparking massive wildfires in California seems to be becoming more common. Pacific Gas & Electric went out of business in 2019 after being found responsible for igniting fires in northern California.

A winter storm December 6, 2018 led to several mudslides and debris flows in the Malibu area, temporarily shutting down several roads, including the Pacific Coast Highway. State Route 23, Bonsall Drive, Kanan Dume Road, and Cuthbert Road were all shut down until cleanup crews could remove mud and debris (CBS Los Angeles, 2018). Boulders even slid onto Topanga Canyon Road, which is outside of the Woolsey Fire burn scar. Additional mudflows occurred January 5, 2019.

The Santa Monica Mountains are adjacent to the Pacific Ocean, so they receive the full effect of frontal storms. Mudslides, landslides, and debris flows all occur regularly. For example, significant debris flows occurred in the Springs fire burn area in 2014, and some of the largest flows in recent recorded history occurred in the area in 1995 following the Green Meadows and Old Topanga fires (WERT, 2018). Efforts to contain the flows have not been consistently successful. According to author John McPhee, “The several debris basins in the Santa Monicas had worked with varying success. People had died in their beds there, buried alive by debris” (McPhee, 2019). Still, these events have not discouraged developers from building here.

Debris flow control structures are heavily relied upon so that highly valuable properties can be packed into mountainside washes. In Trancas Canyon, two debris basins were constructed to protect residents from flash flooding and debris flows along with the channelization of Trancas Canyon Wash next to the neighborhood (Figure 4). Mud can be seen in the concrete section from a debris flow after the Woolsey fire, but these structures were adequate to protect

residents this time. The reward of living by the sea in Malibu must be worth the risk of inundation by mudflows or destruction by debris flows for these residents. With so many wealthy potential buyers in the greater city of Los Angeles, there is likely always a supply of people willing to accept the risks of living directly in the urban-wildland interface.



Figure 4. Image from Google Earth Pro 1/3/2019 following debris flows.

The City of Malibu’s Public Works Department released a “Draft Post-Fire Risk and Vulnerability Map” indicating hazard risk based on theoretical 2-year, 10-year, 25-year, and 50-year storms for the Woolsey Fire burn area (City of Malibu, 2018). They depict the likely flood extent (low-high risk) displayed with parcels, so that at-risk structures could be determined. However, these maps were produced with FLO-2D PRO and HEC-RAS 2D software to show inundation under the assumptions of zero infiltration and entirely blocked storm drains and

culverts. They did not simulate mud or debris flows, which were much more likely to occur but more difficult to model. The USGS released their post-wildfire debris flow assessment, publishing GIS layers for debris flow likelihood, potential volume, and combined hazard (USGS, 2018). This map is based on a design storm with a peak rain intensity of 24 mm/hour. The L.A. County Fire Department and sheriff's department responded by assigning additional resources to areas at risk in preparation for the storm. They anticipated the possibility of power lines being disrupted and residents losing the ability to call 911, so swift-water rescue teams were even put on emergency alert (Hayes et al., 2018). Additionally, the Watershed Emergency Response Team (WERT) produced a detailed report on debris flows in the Santa Monica Mountains, but the final draft was published a week after flows occurred (WERT, 2018).

Improving GIS modeling capabilities at the local level seems likely to improve emergency response in this case. The FLO-2D model used by the City of Malibu is more appropriate for flooding than debris flows. While the USGS hazard model provided a better assessment of likely risk, it was analyzed only for a design storm with a peak rain intensity of 24 mm/hour and was released a month before the storm. If conditions in the watersheds changed during that month or if more accurate rainfall estimates could be predicted closer to the storm event, a more accurate hazard model could have been produced. Equipping the local government with the GIS capabilities to assess this themselves would provide them with more certainty regarding how to allocate resources during hazardous storms.

D. Los Angeles, CA: Station Fire Debris Flows



Figure 5. Debris flow imagery following the Station fire.

The Station Fire in the San Gabriel Mountains in Los Angeles, CA led to debris flows during a storm November 12, 2009. This fire burned 250,000 acres, destroyed 90 homes, and killed 2 firefighters (Daily News, 2017). The debris flows in the winter months following the fire catastrophically destroyed 41 homes and severely damaged a heavily travelled road (Kean & Staley, 2011). Significant debris flows occurred November 12, 2009 and February 6, 2010.

The San Gabriel Mountains are especially prone to debris flows, even in a region characterized by them. They are both increasing in elevation and eroding at rates among the fastest in the world, although they are rising faster than they are eroding (City of Glendale, n.d.). Several active fault lines here, including the infamous San Andreas fault, create their extreme height and slopes. According to John McPhee in “The Control of Nature”:

“The San Gabriels are so steep and so extensively dissected by streams that some watersheds are smaller than 100 acres. The slopes average sixty-five to seventy per cent. In numerous places, they are vertical. The angle of repose—the steepest angle that loose rocks can abide before they start to move, the steepest angle the soil can maintain before it starts to fail—will vary locally according to the mechanics of shape and strength. Many San Gabriel slopes are at the angle of repose or beyond it. The term “oversteepened” is often used to describe them. At the giddy extreme of oversteepening is the angle of maximum slope. Very large sections of the San Gabriels closely approach that angle. In such terrain, there is not much to hold the loose material except the plants that grow there.” (McPhee, 1989)

Without the protection offered by vegetation following wildfire, soil and ash erodes and tumbles downhill. Slope is among the most important contributing factors to debris flows, so the extraordinarily steep slopes here easily lead to the buildup of dry ravel in the channel bottoms, creating conditions favorable to debris flows. The extreme growth rate and slopes of these mountains leads to their increased rate of disintegration because they are unable to support their own material during a wildfire-debris flow cycle.

Coupled with this is the mountains’ extreme precipitation regime. Precipitation with some of the greatest recorded intensities in the United States has fallen in the San Gabriel

Mountains (McPhee, 1989). Storms moving in from the Pacific Ocean are stalled by the mountains, and orographic lifting can sometimes double the amount of rainfall predicted in the mountains versus in the basins and valleys (City of Glendale, n.d.). This leads to “exceptional” debris flows approximately once a decade, with smaller flows occurring more regularly (McPhee, 1989). With climate change, precipitation may become even more extreme.

However, it does not deter people from living on the alluvial fans the San Gabriels are actively creating either. While erosion may be remarkably fast on a geologic time scale, it may not be fast enough for memories of destructive debris flows to hold in the minds of residents of a bustling city like Los Angeles. Land is so sought after here that even if a few families in a neighborhood move following a debris flow, they can easily be replaced by new immigrants who have yet to be traumatized by such an event.

The City of Los Angeles has gone to great lengths to protect residents from the dangers of debris flows, but disaster still occurs frequently. Many debris control structures have been built in the San Gabriels, like crib structures, which are barriers made of concrete slats (McPhee, 1989). Dams were built to control floods and conserve water, but presently function more as sediment retention basins. These tend to fill up quickly and need to be cleaned out regularly due to the high rate of erosion of the San Gabriels. The washes where they exit the mountains are also typically channelized to control flows and prevent runoff from taking alternate paths on the alluvial fans, which are heavily populated. However, boulders up to 15 miles from the face of the San Gabriel Mountains hint at the historical magnitude of debris flows (City of Glendale, n.d.) and human engineering is regularly overwhelmed by flows much smaller than these.

For example, on Christmas Day, 2003, several debris flows ripped out of the burn scars of the Old Fire and Grand Prix Fire in the San Gabriel Mountains. These flows buried a church

camp in the San Bernardino Forest and killed several people at a KOA campground in Devore, CA. Two people were killed by a debris flow from Cable Canyon and 12 people were killed from a debris flow out of Waterman Canyon (City of Glendale, n.d.). USGS had modeled these areas as being at high risk of experiencing a debris flow. The analysis was distributed to FEMA, the California Office of Emergency Services, and local officials (Bustillo, 2003). Although residents had been warned about the dangers for months, they didn't realize that the risk of debris flows could actually be deadly until disaster struck. Although modeling had been completed in ample time, agencies coordinated with each other efficiently, and residents were warned, the message still fell on deaf ears. Despite the best preparations and intentions, it is not always possible to protect every life when residents insist on remaining in the urban-wildland interface despite warning signs from nature as well as government officials.

Examples of deadly debris flows from the San Gabriel Mountains are abundant. In 1934, debris flows in La Crescenta from the Pickens Fire struck 2 minutes after midnight on New Year's Day, leading to nearly 100 fatalities (City of Glendale, n.d.). In 1969, the Canyon Fire led to 73 fatalities in Glendora, CA. The Kinneloa Fire led to deadly debris flows in Altadena in 1993 and Bailey Canyon in 1994. None of these disasters have prevented people from living directly in the front country of the San Gabriel Mountains where these debris flows occur.

The Station fire of 2009 burned 250,000 acres of the San Gabriel Mountains in prime debris flow country. Although officials had mapped debris flow risk from this fire, a "surprise" storm caused mud and debris flows in La Cañada Flintridge, CA before residents could be evacuated (City of Glendale, n.d.). While there was only a forecast for light rain within the region, a storm cell developed over a small area of the Station fire burn scar, producing debris

flows in a neighborhood that had been assessed as highly vulnerable. The debris basin that had been constructed to protect residents filled within 15 minutes.

Mudflows and debris flows continued to be a problem throughout the winter. On February 6, 2010, 4 inches of rain fell over the burn scar, triggering mudflows that overwhelmed the Mullally Debris Basin in Paradise Valley (O’Neil, 2010). Despite months of time to prepare for this event following the initial debris flows out of the Station fire burn area, a lack of coordination between federal and county officials left La Cañada unprepared. Los Angeles County Public Works was not allowed to implement mudslide protective measures on federal property (O’Neil, 2010). Although Governor Arnold Schwarzenegger visited the neighborhood and promised to expedite a permit for a fourth dumping site for the mud and debris, the damage had already been done. Interagency coordination and preventative rather than reactionary policies are necessary to protect the public from destructive natural disasters like these.

Experts had been able to accurately model the risk of debris flows from specific canyons and had contingency plans in place, but it was not enough to protect residents (Cannon, Perry, & Staley, 2010). An over-reliance on predictive modeling and human engineering may create a false sense of security where residents expect government officials to be able to control nature. However, in mountains that literally create their own weather, not all precipitation events can be predicted. Furthermore, the engineered debris basin was not nearly adequate at holding back debris due to mismanagement by government officials. Debris basins must be both designed with sufficient capacity for large storms and be cleaned out in anticipation of them. Flood frequency data is based on only the limited time colonizers have lived in Los Angeles. Furthermore, climate change is shifting the “normal” flood frequency of the region by making wet and dry periods more extreme (Swain et al., 2018). This is likely to increase the frequency of larger storms.

Cities may also have a budgetary incentive to design for the smaller 20-or-so year floods rather than a 100-year flood, and plan to pay out residents when their homes get destroyed. Stronger intergovernmental coordination, thorough education of the public, and designing debris basins for much greater capacity would likely be beneficial.

Data

Study Areas:

Study Fires for Debris Flow Hazard Analysis

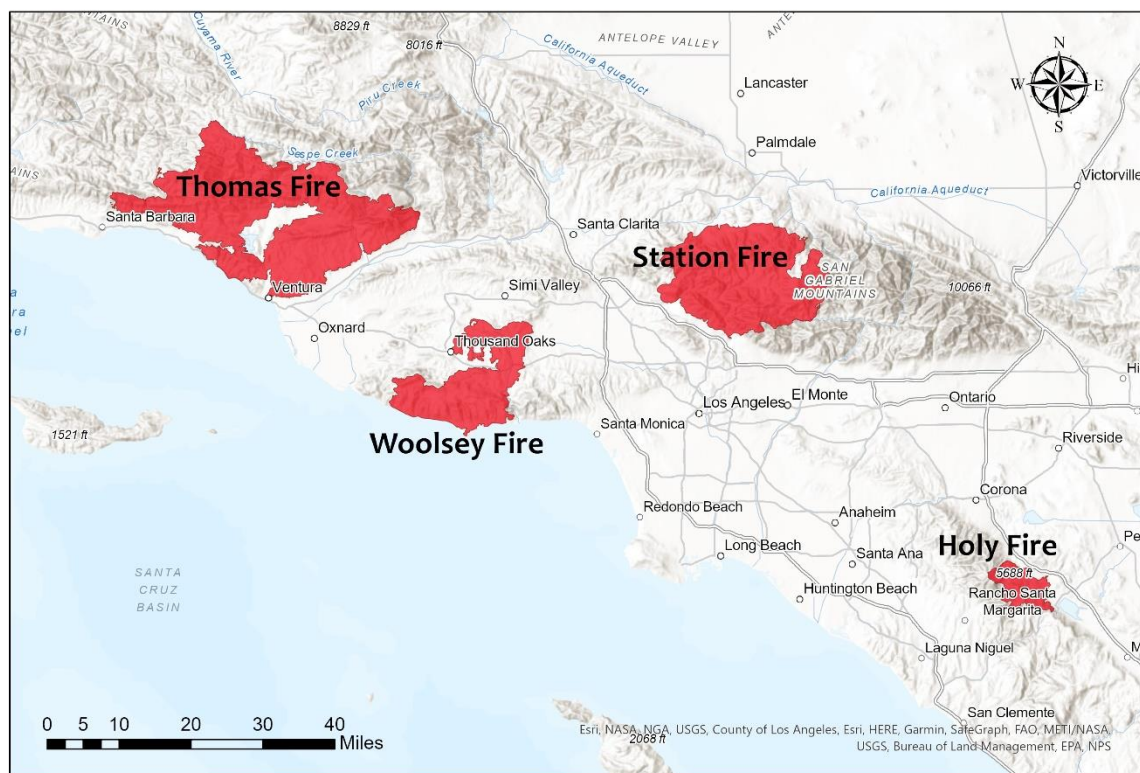


Figure 6. These four fires in Southern California will be used to analyze variables responsible for subsequent debris flows.

Important Dates:

1) Thomas Fire

- Burn Dates: 12/4/2017 – 3/22/2018
- Debris Flow Date: 1/9/2018

2) Holy Fire

- Burn Dates: 8/6/2018 – 9/13/2018
- Debris Flow Dates: 11/29/2018, 12/6/2018

3) Woolsey Fire

- Burn Dates: 11/8/2018 – 11/21/2018
- Debris Flow Date: 12/6/2018, 1/5/2019

4) Station Fire

- Burn Dates: 8/26/2009 – 10/16/2009
- Debris Flow Date: 11/12/2009, 2/6/2010

5) Old and Grand Prix Fires

- Burn Dates: 10/21/2003 – 11/2/2003
- Debris Flow Date: 12/25/2003

Data File Names:

A) Digital Elevation Models (DEMs)

DEMs were downloaded from USGS at viewer.nationalmap.gov/basic:

- USGS_13_n34w118.tif
- USGS_13_n35w118.tif
- USGS_13_n35w117.tif
- USGS_13_n35w119.tif
- USGS_13_n35w120.tif

B) Satellite Imagery

Sentinel imagery was used for the Thomas Fire, Holy Fire, and Woolsey fire, which was downloaded at apps.sentinel-hub.com/eo-browser. Landsat images were used for the Station Fire. These were downloaded at earthexplorer.usgs.gov.

1. Thomas Fire

Pre-Burn: L1C_T11SKU_A012794_20171203T184735.zip

Pre-Debris Flow: L1C_T11SKU_A004386_20180107T184933.zip,

L1C_T11SKU_A013080_20171223T184759.zip

Post-Debris Flow: L1C_T11SKU_A013366_20180112T184725.zip

2. Holy Fire

Pre-Burn: L1C_T11SMT_A007346_20180802T184411.zip

Pre-Debris Flow: LC08_L1TP_040037_20181128_20181211_01_T1.tar.gz

Post-Debris Flow: LC08_L1TP_040037_20181128_20181211_01_T1.tar.gz

3. Woolsey Fire

Pre-Burn: L1C_T11SLT_A017613_20181105T183750.zip

Pre-Debris Flow: L1C_T11SLT_A017899_20181125T184144.zip

Post-Debris Flow: L1C_T11SLT_A009491_20181230T183754.zip,

L1C_T11SLT_A018185_20181215T184316.zip

4. Station Fire

Pre-Burn: LT05_L1TP_041036_20090806_20160907_01_T1.tar.gz

Pre-Debris Flow: LT05_L1TP_041036_20091110_20160903_01_T1.tar.gz

Post-Debris Flow: LT05_L1TP_041036_20091126_20160903_01_T1.tar.gz

5. Old and Grand Prix Fires

Pre-Burn: LT05_L1TP_040036_20030916_20160914_01_T1.tar.gz,

LT05_L1TP_040036_20031002_20160915_01_T1.tar.gz

Pre-Debris Flow: LT05_L1TP_040036_20031119_20160914_01_T1.tar.gz

Post-Debris Flow: LT05_L1TP_040036_20040122_20160914_01_T1.tar.gz

Methods

Pre-Processing:

DEMs:

For each of the four study fires, DEMs were first downloaded from USGS at 1/3 arc-second resolution. Bounding boxes for these study sites were created in ArcGIS Pro using pre-

existing fire maps available in the ESRI Online Portal. DEMs were clipped to the bounding boxes, projected into a custom coordinate system designed for this region, and mosaicked together when multiple DEMs were needed for a single fire. They were resampled using the bilinear interpolation method and given output cell sizes of 10m. The custom projection is based on the Geographic Coordinate System NAD 1983. Parameters are as follows:

Coordinate System Details		✕
Projected Coordinate System	NAD 1983 Southern California Fire Zone (Meters)	
Projection	Lambert Conformal Conic	
WKID	0	
Authority		
Linear Unit	Meters (1.0)	
False Easting	2000000.0	
False Northing	500000.0	
Central Meridian	-118.1	
Standard Parallel 1	33.7	
Standard Parallel 2	34.5	
Scale Factor	1.0	
Latitude Of Origin	33.5	

Output DEMs to be used in the analysis are: Thomas_DEM, Holy_DEM, Station_DEM, and Woolsey_DEM.

Delineating Watersheds

Watersheds had to be delineated for each burn area in order to study debris flows at the scale from which they may cause destruction to life, property, and infrastructure. Output DEMs created for each fire from downloaded USGS files are the initial input for this work sequence. A flow direction raster is produced from the DEM once sinks are filled, and this raster is then used as an input to create the flow accumulation raster. Pour points need to be defined next in a new feature class. A pour point is the outlet for water flow in a given area, and is the lowest point

along the boundary of a watershed (ArcGIS Pro 2.7, 2021). The stream order from which pour points are designated can determine the size of the watershed that delivers flow to them. Pour point locations for these fires were chosen to identify places where debris flows could flow out of the mountains and across a major road or into a neighborhood. This scale of delineation was not fine enough for some of the large watersheds, so they were further split to isolate side canyons contributing to larger streams. This is necessary to get more specific average index values for areas that produce debris flows. Additionally, if watershed debris flow maps had already been created (as in the case of the Thomas Fire), they were georeferenced and watersheds were delineated to match them. Pour point features were created by digitizing points on top of flow accumulation lines. Flow accumulation lines are in raster format and cells hold values representing how many cells contribute flow to them, so values increase downstream along the lines. The further downstream a pour point is digitized along a flow accumulation line, the larger the resulting watershed will be. Pour points and the flow direction raster are the inputs for the watershed tool, which results in a polygon feature class outlining the areas where all cells contribute flow to a given pour point. These watersheds were then used as zones to analyze average index values.

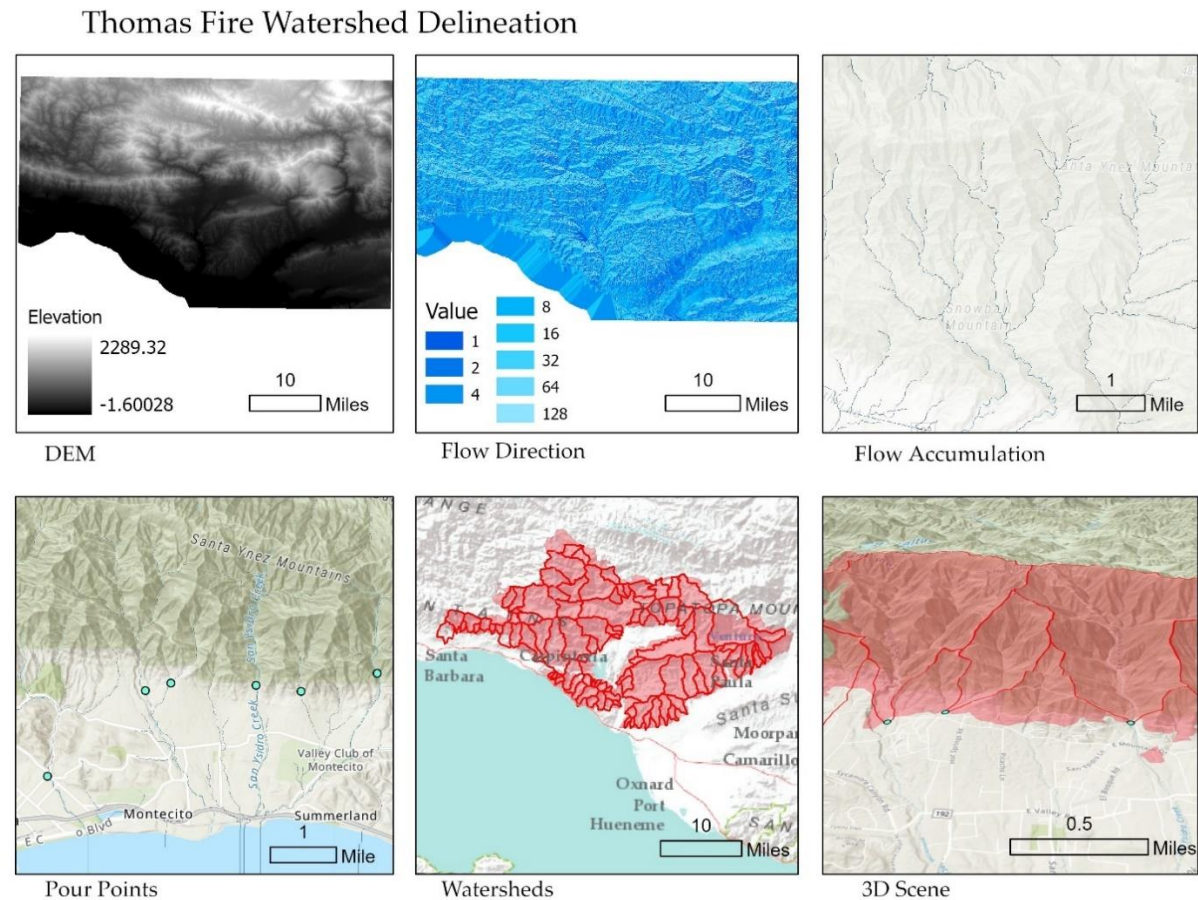


Figure 7. Watershed delineation steps for the Thomas Fire. Pour points were created by layering the flow accumulation raster with a basemap and selecting locations where flow might cross major roads or enter neighborhoods.

Satellite Imagery:

Landsat 5 TM imagery for each fire needed to first be calibrated for radiance, which is the reflectance at the top of the atmosphere. Bands 1 – 5 and Band 7 were calibrated individually and saved as separate files. The satellite sensor is input during this step, along with the date of acquisition and the sun elevation in degrees. Bands were then stacked into a single image, average wavelengths of each band were updated in the metadata, and the files were converted to BIL format to prepare them for atmospheric correction. To develop surface reflectance images

that are free of atmospheric effects, FLAASH is used. Sensor type is input, along with ground elevation, pixel size, flight date, and flight time. The Urban aerosol model, U.S. Standard atmospheric model, and 2-Band (K-T) aerosol retrieval type was used with an initial visibility setting of 40km. Once multispectral settings were set, the tool was run and atmospheric correction computed. All Landsat imagery was processed up to the BIL format step. Due to limited time availability with NAU's FLAASH license, only one image was atmospherically corrected. The rest of the images were instead re-downloaded already atmospherically corrected for the Station Fire.

Sentinel satellite imagery was preferred due to its higher spatial resolution. Four visible and near-infrared bands have a resolution of 10m, while six red edge and shortwave infrared bands have a resolution of 20m. ENVI Classic cannot easily work with these types of files, so SNAP (SeNtinel Applications Platform) was used to process these images instead.

Atmospherically corrected Sentinel images were downloaded for the Thomas, Holy, and Woolsey fires. The steps and tools used are very similar in ENVI and SNAP for the next processes that were performed on the imagery: band math to create indices commonly used in remote sensing to study post-wildfire debris flows.

Remote Sensing Indices:

Satellite images were pre-processed for radiometric calibration and atmospheric correction before being used in band ratios. The following band ratios (remote sensing indices) were calculated using atmospherically corrected imagery for each fire: NDVI (Normalized Differenced Vegetation Index), BSI (Bare Soil Index), dNBR (differenced Normalized Burn Ratio), and NDSI (Normalized Difference Soil Index). These were analyzed by mean value at the

watershed scale to determine their correlation with debris flows. Each index was calculated according to the following formulas using band math in either ENVI or SNAP:

$$\text{NDVI} = (\text{NIR} - \text{RED}) / (\text{NIR} + \text{RED})$$

$$\text{NBR} = (\text{NIR} - \text{SWIR}) / (\text{NIR} + \text{SWIR})$$

$$\text{NDSI} = (\text{GREEN} - \text{BLUE}) / (\text{GREEN} + \text{BLUE})$$

$$\text{BSI} = ((\text{SWIR} + \text{RED}) - (\text{NIR} + \text{BLUE})) / ((\text{SWIR} + \text{RED}) + (\text{NIR} + \text{BLUE}))$$

The dNBR is calculated by subtracting the pre-debris flow NBR from pre-burn NBR, but other index values were calculated by directly following the above formulas. Landsat and Sentinel satellites have different bands that correspond to each of the inputs, so care was taken to ensure the right band math was used to calculate index values for each image. Once index values were created for each fire, these output raster files were used as inputs in Python codes to generate mean statistics at the watershed level and update these values into the watershed attribute tables.

Other Variables

Several other variables were considered significant in potentially leading to debris flows. Soil data that had been field-surveyed and was available to download was used to compare with remotely sensed soil data. A significant amount of data is available through the Natural Resources Conservation Service through the United States Department of Agriculture. Data was downloaded in a gNATSGO package in the form of related tables and a Python toolkit. These could be used to generate over 200 unique soil maps for any state (in this case, California).

Categories include soil chemical properties, soil health properties, soil physical properties, vegetative productivity, and wildlife management. For this study, raster maps for each study fire were created for variables K factor (whole soil), K factor (rock free), and percent clay content of the soil.

The hypsometric integral of each watershed was calculated using a script written in Python (Appendix 2.4). This value approximates the overall slope of the watershed and was strongly correlated with debris flow occurrence in the study on debris flows in Montecito following the Thomas Fire (Cui et al., 2019). The hypsometric integral uses the following formula to compare the maximum, minimum, and average elevation of a watershed to produce a single representative number:

$$HI \approx \frac{H_{ave} - H_{min}}{H_{max} - H_{min}}$$

where H_{ave} is the average elevation value of a watershed, H_{min} is the minimum elevation value of a watershed, and H_{max} is the maximum elevation value of a watershed.

A combination of slope with burn severity has a strong correlation with debris flow occurrence. To analyze these variables, slope rasters for each study site were reclassified into Boolean rasters with values of 1 representing slopes greater than 23 degrees. Both dNBR and BAER field-verified burn severity data was also reclassified into Boolean rasters with values of 1 representing moderate or high-severity burns. BAER data was not available for every fire. These Boolean rasters were multiplied together so that the proportion of a watershed with slopes in excess of 23 degrees and burned at moderate to high severity was determined for each watershed of each fire. These values were updated into the watershed attribute tables with a separate field for BAER burn data where available. This way, remotely sensed burn severity data could be directly compared with field-verified burn data.

List of Variables:

- Hypsometric Integral
- Mean dNBR
- Mean NDVI
- Mean NDSI
- Mean BSI
- Mean Slope
- Proportion of watershed with slope > 23 degrees and burned at moderate or high severity (from dNBR)
- Proportion of watershed with slope > 23 degrees and burned at moderate or high severity (from BAER)
- K Factor (whole soil)
- K Factor (rock-free)
- Percent Clay content of soil

Python Scripting

Each of the variables above were analyzed at the watershed scale with scripts written in Python. Here I will discuss basic principles and approaches used for each unique script. For the complete codes with comments explaining each line, please see Appendix 2.

The general methodology is to open a Python graphic user interface (GUI), which enables writing, editing, and running of scripts. For this project, I used PythonWin. The first step is to import the Python site package ArcPy, which contains all of the tools available in ESRI's GIS

software (ArcMap and ArcGIS Pro). The default workspace should be set to the geodatabase where input files are located. Because this project worked primarily with rasters, the spatial analyst license needed to be checked out and all functions of this extension needed to be imported separately in the next step. Input rasters and the name of the variable to be calculated (written into a new field in the watershed attribute table) are held as variables to simplify future lines of code. The code then checks if the new field already exists in the watershed attribute table, and if it does not, it creates it. An update cursor is next used to write values of each variable into the attribute table of the watershed feature class for each watershed. Loop structures enable iteration through each feature in a feature class. The block of code for the variable being calculated is included in a loop structure for this update cursor. Values are printed into an interactive window so progress can be seen while the code is running. Once the code has written values for all watersheds into the attribute table, it proceeds to the last section. The spatial analyst license is checked back in and a message is printed letting the user know the task has been completed.

While this approach is consistent for all the codes I used and most of the individual lines of code are the same, calculating the values of these variables can be more complicated. Calculating the mean index value (Appendix 2.1) is relatively simple. The ‘Extract by Mask’ tool is used to extract a raster of the index in the shape of the watershed. The mean value of this output raster is then calculated and written into the attribute table before the cursor moves to the next row / watershed. Mean K Factor (Appendix 2.2) and percent clay (Appendix 2.3) are also calculated this way, but first require reclassification of the raster produced by the Gridded National Soil Survey Geographic Database (gNATSGO) from the USDA.

In calculating the hypsometric integral (Appendix 2.4), ‘Extract by Mask’ is also used. A DEM is used as the raster to extract data from in this code. The minimum, maximum, and average elevation values are calculated for each watershed once data has been extracted according to the shape of the watershed. The line “ $HI = (H_{ave} - H_{min}) / (H_{max} - H_{min})$ ” calculates the hypsometric integral, where H_{ave} is the average, H_{min} is the minimum, and H_{max} is the maximum elevation of the watershed.

The codes calculating the proportion of the watershed burned at moderate or high severity and with slopes in excess of 23 degrees from dNBR (Appendix 2.5) and from field-verified BAER data (Appendix 2.6) are more complicated. ‘Extract by Mask’ is used on both the burn severity raster and the slope raster. The slope raster is reclassified into a Boolean raster where 1 represents slopes greater than 23 degrees and 0 represents slopes 23 degrees or less. The dNBR and BAER rasters are also reclassified into Boolean rasters. BAER rasters are reclassified so values of 3 or 4 are given the value of 1 and all other values 0, and dNBR rasters are reclassified so values greater than or equal to 0.27 become 1 and all other values 0. The reclassified slope and burn severity rasters are then multiplied together. In the output raster from this step, values of 1 represent places where both conditions are true. The number of cells with value of 1 are counted and multiplied by the area of each cell to determine the total area in the watershed with high slope and a moderate or severe burn. This is divided by the total area of the watershed to determine the final proportion that is written into the watershed attribute table.

The general approach for calculating variables within a watershed and writing values into an attribute table will be the same no matter what is being calculated specifically. These lines of code can be copied and pasted into new codes. The blocks within the loop structure of the update cursor need to be changed depending on the calculation required. These codes could be useful in

future studies of watersheds unrelated to debris flows as well, so use of my codes is strongly encouraged.

Debris Flow Identification

Scientific literature, online videos, and news articles were used to identify the occurrence of debris flows in certain watersheds, canyons, across roads, or into neighborhoods. If maps of known debris flows can be found in the scientific literature, they were georeferenced into ArcGIS Pro. This was done for the Thomas Fire based on Figure 9 by Cui, Cheng, and Chan (Cui et al., 2019). Only debris flows from the first storm that produced them were included in the analysis.

Debris flows were also identified using Google Earth Pro imagery overlaid with watershed boundaries for each fire where possible. Debris flows are commonly identified using high resolution imagery (Sensing et al., 2017), higher than the downloaded imagery used for creating index values. Google Earth Pro often has imagery with less than 1 foot resolution, so changes in smaller features rather than just changes in pixel color can be seen, aiding in the ability to visually identify debris flows. For large debris flows, identification is very obvious (Figures 3 and 4). However, smaller debris flows, mudflows, or highly turbid flash floods are exceptionally difficult to differentiate. Furthermore, imagery may not be available for the dates or locations necessary for the analysis. Imagery availability is expected to improve as more satellites go into orbit in the future.



Figure 8. Google Earth Imagery of a debris flow from San Ysidro Creek Watershed. The top image is from 12/30/2017 and the bottom from 1/12/2018 following the 1/9 debris flow. Deposition can clearly be seen downstream from the delineated watershed in the middle of the bottom image.

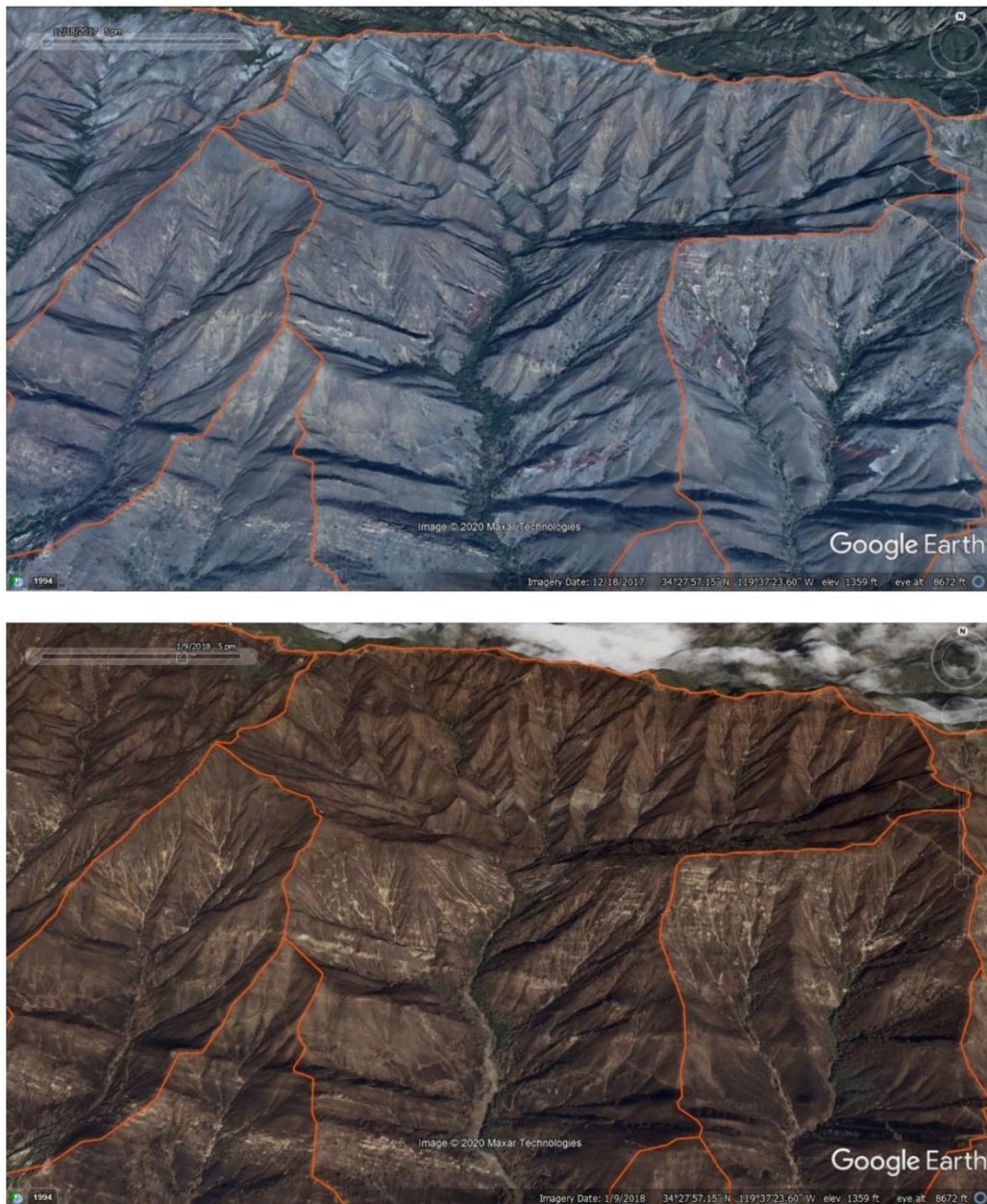


Figure 9. Google Earth Imagery of incision in San Ysidro Creek Watershed before and after the 1/9/2018 debris flow. Locations of abrupt changes in slope are often where debris flows shift from being depositional (Figure 8) to incisional.

Comparing the Variables in Regression

Debris flows were converted to Boolean values with '1' representing a debris flow within a watershed and '0' indicating no debris flow was identified. This was done for each of the four study fires. All potential explanatory variables were included in OLS regression for each fire. If variables were found to be redundant or statistically insignificant, they were removed and OLS was performed again. This process was repeated until the most statistically significant variables remained.

Results

Remote Sensing:

Remote sensing indices produced for each fire are displayed below. The timing of passing satellites was extremely important, as many factors could render a satellite image useless for analysis. Cloud presence could either cover the data completely by hiding areas of interest or potentially obscure data through wispy vapors. Snow, shadows, or smoke from actively burning fires could also impede data collection. Fires that burned more recently had more satellite images available due to more satellites covering Earth. Data availability is likely to improve in the future as even more satellites are added and temporal resolution is increased. Results from the remote sensing portion of this project are included below.

Thomas Fire Remote Sensing Indices

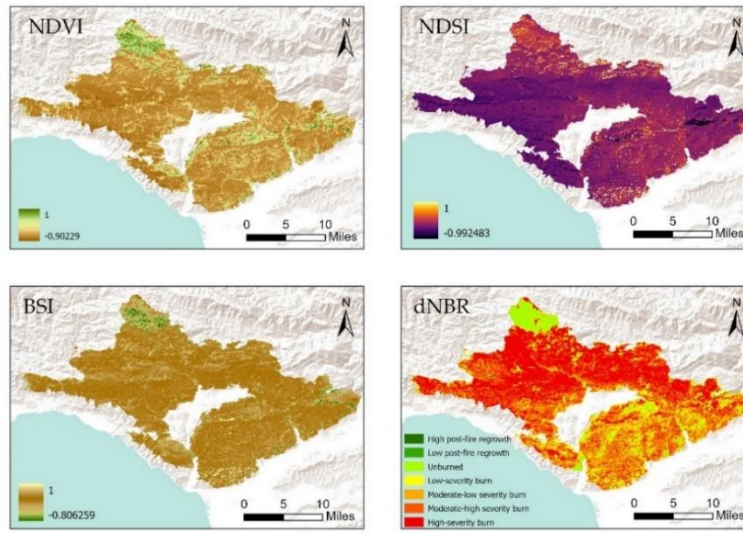


Figure 10. Thomas Fire Remote Sensing Indices. NDVI, NDSI, BSI, and dNBR calculated from pre-debris flow Sentinel imagery.

Woolsey Fire Remote Sensing Indices

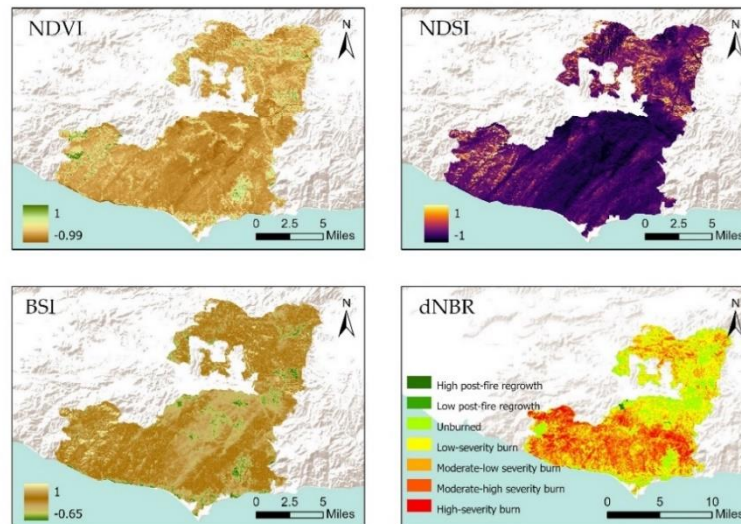


Figure 11. Woolsey Fire Remote Sensing Indices. NDVI, NDSI, BSI, and dNBR calculated from pre-debris flow Sentinel imagery. Thin clouds present on this image date limits its accuracy, especially at lower wavelengths. Cloud interference is especially noticeable in the dark streaks of the NDSI image.

Holy Fire Remote Sensing Indices

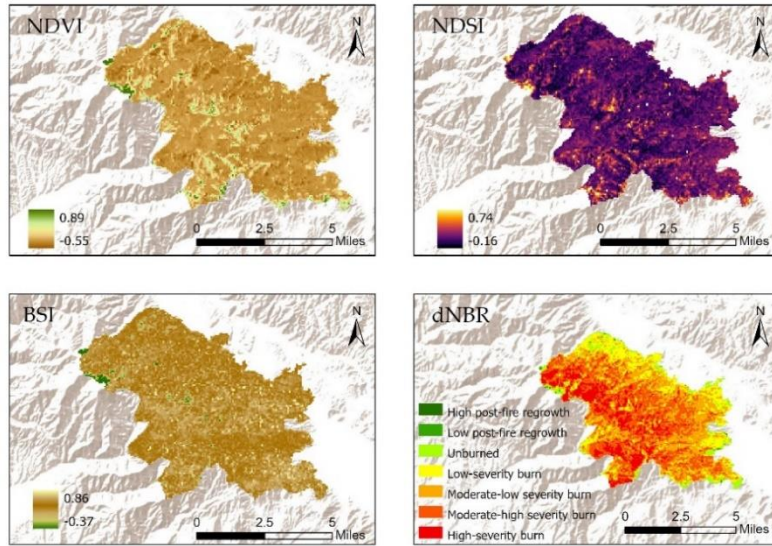


Figure 12. Holy Fire Remote Sensing Indices. NDVI, NDSI, BSI, and dNBR calculated from pre-debris flow Sentinel imagery.

Station Fire Remote Sensing Indices

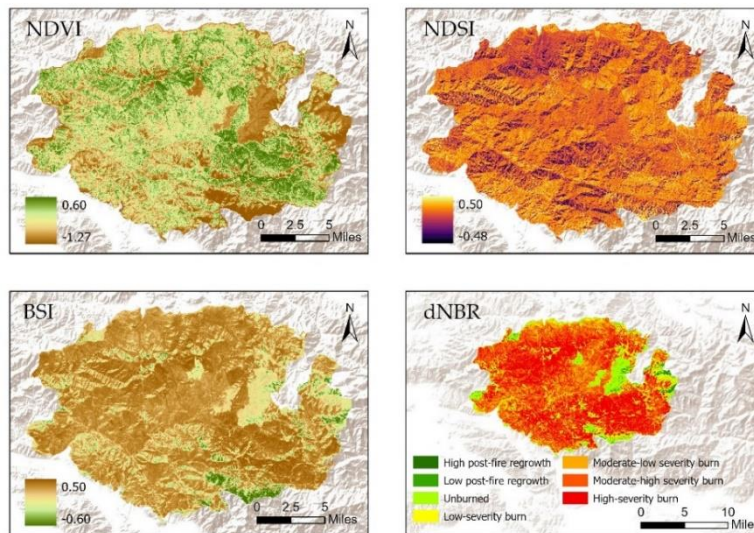


Figure 13. Station Fire Remote Sensing Indices. NDVI, NDSI, BSI, and dNBR calculated from pre-debris flow Landsat imagery. The San Gabriel Mountains where this fire took place are extremely steep, so it is possible that dark shadows from the peaks distorted some of this data. It does not make sense for NDVI to be high in the same place as a high-severity burn.

Regression:

An ordinary least squares regression analysis was performed on all variables for each fire. Insignificant and redundant variables were removed and the analysis performed multiple times until the best-fit model for each fire could be determined. Without high resolution rainfall intensity data, datasets could not be combined to analyze variables from all study locations at once. Furthermore, equations produced by ordinary least squares regression would not be reliable models to use for debris flow prediction without this precipitation data. However, this process was effective for illuminating which variables are statistically significant in leading to debris flows in mountain ranges of Southern California.

Summary of OLS Results - Model Variables

Variable	Coefficient [a]	StdError	t-Statistic	Probability [b]	Robust_SE	Robust_t	Robust_Pr [b]	VIF [c]
Intercept	0.487940	0.242293	2.013838	0.045925*	0.210309	2.320105	0.021761*	-----
MEAN_DNBR	-1.685386	0.321541	-5.241585	0.000001*	0.274654	-6.136403	0.000000*	2.734577
PREFD_NDSI	-2.049346	0.530316	-3.864384	0.000176*	0.473121	-4.331552	0.000031*	1.089258
BAER_23	1.248586	0.217183	5.749004	0.000000*	0.174551	7.153149	0.000000*	2.463880
MEAN_KF_WS	1.663849	0.445577	3.734141	0.000281*	0.375468	4.431400	0.000021*	1.422920

Figure 14. Summary of OLS Results from the Thomas Fire following removal of insignificant variables.

Results from the Thomas fire indicate statistically significant results for the mean dNBR, mean NDSI, the mean K factor (whole soil), and the proportion of the watershed burned at moderate or high severity (from BAER) and with slopes in excess of 23 degrees (Figure 14). Robust probabilities had to be analyzed because the Koenker Statistic was statistically significant. For debris flows in the Holy Fire burn area, mean K factor (whole soil) and mean

NDSI were found to be significant. For debris flows in the Woolsey Fire burn area, mean NDSI, BSI, NDVI, percent clay, and ‘the proportion of the watershed burned at moderate or high severity (from remotely sensed dNBR) with slopes in excess of 23 degrees’ were significant variables. In the Station fire burn scar, mean NDSI and ‘the proportion of the watershed burned at moderate or high severity (from remotely sensed dNBR) with slopes in excess of 23 degrees’ were significant variables leading to debris flows.

It is interesting to note that the rock-free / fine fragments K factor (Kf) was never a significant variable, but whole soil K factor (Kw) consistently was. The USGS model does use Kf rather than Kw, likely because debris flows require an abundance of fine-grained material for initiation (Costa, 1984). Larger rocks in the soil do not contribute to the initiation of a debris flow, but can only be carried once sufficient fine-grained material has been mobilized. The presence of rocks in soil will be inconsistent regionally and their erodibility is not as important as the erodibility of the fine soil fragments, so the use of Kf rather than Kw in the USGS’s hazard model seems warranted. Comparing these values to the soil’s parent material might illuminate answers as to why the Kw was found to be a more significant variable for these fires.

Additionally, high burn severity at high slopes was statistically significant. Soil is less stable on severe slopes, especially following wildfire. Ash and debris is more likely to slide off steep slopes as dry ravel, providing the large supply of fine material needed to initiate a debris flow. Burn data from BAER where available was more reliable than the remotely sensed dNBR to determine burn severity. The spectral signature of plant material following wildfire varies with vegetation type (Staley et al., 2018), so scientists in the field can better estimate burn severity than a single remote sensing index can. For example, chaparral environments in southern California often have significant amounts of grass, which produces a high dNBR value when

burnt but low burn severity (Staley et al., 2018). Physically walking this environment can provide the clarity for how to interpret dNBR values based on vegetation type. While dNBR is an adequate variable to include in a predictive hazard model for debris flows, field-verified data is preferred.

Results also indicate that NDSI would likely be a good variable to include in a model like this because of its consistent statistical significance across multiple fires. It is a soil brightness index, so it can also identify severely burned areas based on how darkly charred the soil has become. However, more data is currently needed to incorporate this variable into an existing hazard model.

Ordinary least squares regression of the Thomas, Holy, Woolsey, and Station fires indicate mean dNBR, mean NDSI, mean K factor (whole soil), and the proportion of the watershed burned at moderate or high severity (from BAER) and with slopes in excess of 23 degrees are important variables to use in a debris flow hazard model (Appendix 3). If precipitation intensity data were added to this analysis, a model could be produced to predict debris flow hazard throughout the mountains of Southern California. This rainfall data might also help clarify discrepancies for why certain variables exhibited stronger local importance than others. Regardless, variables found to be significant in this Southern California analysis largely align with those used by the USGS. The USGS Western Preliminary Hazard Assessment Model is a strong choice for predictive debris flow modeling in Southern California, which relies on dNBR, severely burned areas at high slopes from BAER data, the soil K factor (Kf), watershed elevation range, and precipitation intensity.

Discussion

Case studies of debris flows from the Thomas, Woolsey, Holy, and Station fires have demonstrated the need for improved GIS modeling capabilities at the local level. Python scripts can utilize the site package ArcPy to import all the tools available for spatial analysis in ArcMap or ArcGIS Pro. Scripts can be written to streamline complicated GIS work sequences or to perform functions not available in the included toolboxes. I wrote 6 unique codes for this debris flow analysis that would be useful for local governments interested in modeling hazard independently. A couple of additional steps would be required before these could be used to run the USGS hazard model, including incorporating rainfall and debris volume estimates. However, the codes that calculate the mean dNBR, mean Kf factor, and the proportion of the watershed burned at moderate or high severity and with slopes in excess of 23 degrees could be used immediately. Modeling could feasibly be conducted at the local level utilizing the most recent burn severity and forecasted precipitation data.

Advanced modeling had only been completed two days before debris flows occurred in Montecito, so there was not sufficient time to either evacuate residents or properly educate them regarding the dangers of debris flows before they occurred (Garcia et al. 2018). In the cities of Lake Elsinore and Corona, emergency response to debris flows from the Holy fire burn scar may have been improved by shutting down roads that were at high risk of being impacted ahead of time. Reactionary responses cause more danger to residents. These closures could have been updated on databases serving smartphone navigation apps to re-route individuals and improve traffic flow. In the case of the Malibu debris flows following the Woolsey fire, the City of Malibu published hazard maps from flood inundation models rather than debris flows, the more likely process to occur given the substantial sediment supply in canyons of the Santa Monica

Mountains following the Woolsey fire. While the USGS had already published a hazard map, an ability to run this model at the local level themselves could have improved prediction certainties because the most up-to-date burn severity data and precipitation forecasts could have been used. GIS technology has the potential to mitigate risk from debris flows, but only if it is effectively utilized as a tool.

Communication is also exceptionally important for mitigating potential damage from debris flows. People that live in or visit areas likely to undergo these hazards need to be properly educated about the risks. Following the Thomas fire, many Montecito residents were warned about potential debris flows, but did not realize they could be deadly or their probability of occurrence. Similarly, people of Los Angeles had been warned for months that areas downstream of the Old fire and Grand Prix fire burn scars were highly susceptible, but many did not realize the danger until deadly debris flows occurred on Christmas Day of 2003. Hazard communication has clearly not been effective enough. Disseminating maps both online and in public places with descriptive information about debris flow qualities as well as contributing factors would likely be helpful. Additionally, certain communities are more vulnerable than others and may require extra effort to be warned. Redundancy in warning systems is necessary and should include all languages spoken by a significant portion of the population. Warnings should be promoted through radio, television, smartphones, and possibly with siren alert systems to ensure messages reach as many people as possible and are taken seriously. The best science and most accurate models in the world will be useless if their findings cannot be adequately communicated with the public.

Coordination among different responding agencies is crucial for efficient hazard response. Many different government agencies are involved during the entire wildfire- debris

flow cycle. Fire departments and BAER teams respond to the initial wildfire, flood control agencies are responsible for cleaning out debris basins in anticipation of an influx of sediment, and several different organizations like WERT, the USGS, and city governments may release hazard maps or models to the public. Additionally, FEMA, the National Guard, and local sheriffs may provide assistance to communities by distributing resources, closing roads, or warning people by going door to door. Swiftwater rescue teams and medical first responders are standing by when the storm lands to be able to assist those in need. Responsibilities need to be clearly outlined and plans established in advance of potentially destructive storms so that resources offered by each organization can be utilized effectively and in a timely manner. Some emergencies can be prevented with proactive planning.

GIS and remote sensing are useful sciences for studying debris flows. Analyzing data remotely can be done with only a couple trained specialists, so is likely less expensive than extensive fieldwork required of more complicated physical debris flow models. Additionally, fieldwork could be impractical for a number of reasons; this past year, COVID-19 presented a significant obstacle to scientific data collection. Modeling still needs to be completed despite any obstacles, and modeling based on remote sensing is an important tool to have. Timeliness of model results could be improved using GIS at the local level by running the USGS debris flow hazard model with some of the Python scripts I wrote.

Despite numerous benefits of conducting science remotely, this methodology was not adequate for designing a new Southern California debris flow hazard model. The biggest obstacle to construction of a model was data accessibility. Rainfall data was not accessible through NOAA after 2014, and for older fires where rainfall data is available, there are fewer satellite images to analyze. This is because there were fewer satellites collecting images of Earth

the further back in time one looks, affecting the ability to create remote sensing images for each fire as well as identifying debris flows in Google Earth Pro. Image viability is often a matter of luck: clouds, smoke from fires, snow, and heavy shadows all obscure data. The San Gabriel Mountains in particular are so steep that shadows make remote sensing much more difficult.

Additionally, identifying the debris flows from Google Earth Pro introduced subjectivity, especially because flows were classified only in the binary “Yes or No”. Post-wildfire discharge from mountain creeks could come in the form of mudflows or sediment-laden flash floods that alter the channel rather than true debris flows. Although I tried to identify them based on visible accumulation of mud or movement of rocks, this was not always possible. Spatial or temporal resolution of Google Earth Pro images along with vegetation in the channel could also obscure signs of debris flows. For example, images of before and after the Christmas debris flows in Devore, CA are a year apart, making it impossible to isolate changes due to debris flows. Older images also have coarser spatial resolution, so smaller changes in the landscape can’t be identified. Overhanging vegetation obscured signs of debris flows in watersheds of the Station fire burn scar on several occasions, but these were able to be positively identified based on news reports or scientific literature.

The potential for GIS modeling capabilities to expand certainly exists. Satellite coverage is expected to increase temporally, with more satellites collecting images of any given location on Earth. With more images fewer days apart, there is a greater likelihood of being able to find acceptable images for remote sensing purposes. Prioritizing data accessibility at the national level would also deeply benefit GIS. This would include processing satellite images to both radiance and reflectance levels for all major satellites and making those images available for download in a timely manner. Although this is currently done for all Landsat images, Europe’s

SentinelHub EO Browser is much more user-friendly than the USGS's Earth Explorer. Rainfall data accessibility is also extremely important for climate science. For unknown reasons, NOAA has not released its hourly precipitation data since 2014. At the time of this writing (March 2021), its website was also down regularly. For modeling capabilities to improve, the highest resolution and most timely data needs to be publicly available. A national data archive or hub for scientists to go to access all published government data would likely be incredibly beneficial in increasing accessibility. Modeling with GIS and remote sensing is another tool to have in the toolkit, so it is worth developing existing knowledge of debris flows with these newer technologies.

Data from OLS regression analysis of variables influencing debris flow initiation in four study fires indicates that the hazard model used by USGS is highly appropriate for Southern California. Variables used in this model for both probability and volumetric predictions were found to be statistically significant for four fires with accompanying debris flows in Southern California from the last 15 years (Appendix 3). Consistent statistical significance of NDSI values with debris flow occurrence suggests this is another remotely sensed variable that could be used in debris flow hazard modeling, although more research with high-resolution rainfall data is necessary to create such a model. Local governments would likely benefit from being able to run the USGS model independently. Since predictions are made based on a single model storm, these predictions would have higher certainty if the model was run with precipitation forecasts from the impending storm concerning local governments. Resources could then be allocated more efficiently to protect residents in basins most likely to experience debris flows based on more accurate precipitation data. Running this model at the local level can be done largely with the Python scripts I wrote for this project, so this would be very feasible to implement if prioritized.

Conclusion

Regular debris flow occurrence has not impeded development of the wildland-urban interface in Southern California. Human populations have crowded onto alluvial fans at the mouths of debris-flow prone washes in major mountain ranges like the San Gabriel and Santa Monica Mountains despite regular deadly events. Severe wildfire, high slope, and winter storms with extreme precipitation intensity are conditions that make debris flow initiation likely. With climate change forecasts predicting larger, more destructive wildfires, and more extreme precipitation patterns, risk to these populations is increasing. There are several ways of mitigating danger by local governments as demonstrated by case studies of debris flows following the Thomas, Holy, Woolsey, and Station fires. Residents must be made aware of the dangers through effective communication via multiple mediums. Improved GIS debris flow hazard modeling capabilities at the local level have the potential to provide the most benefit since outsourced modeling may produce maps displaying hazard either too early or too late to be of practical use. Finally, coordination of emergency response between various government agencies needs to be efficient and transparent, especially for so complex an issue with so many responding organizations. By focusing attention on creating better policy in these three areas, hopefully human life and property can be better protected when the next significant debris flow occurs in Southern California.

References

- Alta Environmental. (2019, November 14). SAR Post-Fire Monitoring Report for the Holy Fire. Retrieved from https://content.rcflood.org/downloads/NPDES/Documents/SA_Other/20191114/SAR_2018%20Holy%20Fire_Post-Fire%20Monitoring%20Report_11.14.2019_FINAL.pdf
- ArcGIS Pro 2.7. (2021). How OLS regression works. Retrieved April 09, 2021, from <https://pro.arcgis.com/en/pro-app/latest/tool-reference/spatial-statistics/how-ols-regression-works.htm>
- ArcGIS Pro 2.7. (2021). How watershed works. Retrieved April 09, 2021, from <https://pro.arcgis.com/en/pro-app/latest/tool-reference/spatial-analyst/how-watershed-works.htm#:~:text=A%20watershed%20is%20the%20upslope,common%20outlet%20as%20concentrated%20drainage.&text=The%20outlet%2C%20or%20pour%20point,the%20boundary%20of%20a%20watershed>
- Associated Press. (2021, January 26). SoCal Edison to pay \$2.2-billion settlement in Deadly 2018 Woolsey fire. Retrieved March 28, 2021, from <https://www.latimes.com/world-nation/story/2021-01-26/utility-to-pay-2b-settlement-in-deadly-2018-california-fire>
- Billmire, M. E., Elliot, M. J., Endsley, W. J., & Robichaud, K. A. (2015). Rapid response tools and datasets for post-fire modeling: linking Earth Observations and process-based hydrological models to support post-fire remediation. *Remote Sensing & Spatial Information Sciences*, (7), 469–476. <https://doi.org/10.5194/isprsarchives>
- Billmire, M. E., Elliot, M. J., Endsley, W. J., & Robichaud, K. A. (2015). Rapid response tools and datasets for post-fire modeling: linking Earth Observations and process-based hydrological models to support post-fire remediation. *Remote Sensing & Spatial Information Sciences*, (7), 469–476. <https://doi.org/10.5194/isprsarchives>
- Bisson, M., Favalli, M., Fornaciai, A., Mazzarini, F., Isola, I., Zanchetta, G., & Pareschi, M. T. (n.d.). *A rapid method to assess fire-related debris flow hazard in the Mediterranean region: An example from Sicily (southern Italy)*. <https://doi.org/10.1016/j.jag.2005.04.003>
- Blair, T. C., & Associates, B. (n.d.). *Cause of dominance by sheetflood vs. debris-flow processes on two adjoining alluvial fans, Death Valley, California*.
- Cannon, S., Perry, S., Staley, D. (2010). Lessons learned from an emergency release of a post-fire debris-flow hazard assessment for the 2009 Station fire, San Gabriel Mountains, southern California. *Ui.Adsabs.Harvard.Edu*. Retrieved from <https://ui.adsabs.harvard.edu/abs/2010AGUFMNH44A..05C/abstract>
- Chen, L., Sela, S., Svoray, T., & Assouline, S. (2013). The role of soil-surface sealing, microtopography, and vegetation patches in rainfall-runoff processes in semiarid areas. *Water Resources Research*, 49(9), 5585–5599. <https://doi.org/10.1002/wrcr.20360>

- Costa, J. E. (1984). Physical geomorphology of debris flows. *Developments and Applications of Geomorphology*, 268–317. https://doi.org/10.1007/978-3-642-69759-3_9
- Cui, Y., Cheng, D., & Chan, D. (2019). Investigation of post-fire debris flows in Montecito. *ISPRS International Journal of Geo-Information*, 8(1). <https://doi.org/10.3390/ijgi8010005>
- Deng, Y., Wu, C., Li, M., & Chen, R. (2015). RNDSI: A ratio normalized difference soil index for remote sensing of urban/suburban environments. *International Journal of Applied Earth Observation and Geoinformation*, 39, 40–48. <https://doi.org/10.1016/j.jag.2015.02.010>
- Elkadiri, R., Sultan, M., Youssef, A. M., Chase, R., Bulkhi, A. B., & Al-Katheeri, M. M. (2014). A Remote Sensing-Based Approach for Debris-Flow Susceptibility Assessment Using Artificial Neural Networks and Logistic Regression Modeling. *IEEE JOURNAL OF SELECTED TOPICS IN APPLIED EARTH OBSERVATIONS AND REMOTE SENSING*, 7(12). <https://doi.org/10.1109/JSTARS.2014.2337273>
- Gartner, J. E., Cannon, S. H., Santi, P. M., & Dewolfe, V. G. (2008). Empirical models to predict the volumes of debris flows generated by recently burned basins in the western U.S. *Geomorphology*, 96(3–4), 339–354. <https://doi.org/10.1016/j.geomorph.2007.02.033>
- Goto, E. A., Gray, S., Keller, E., & Clarke, K. C. (2021). *Using Mixed-Methods to Understand Community Vulnerability to Debris Flows in Montecito, CA*. https://doi.org/10.1007/978-3-030-60227-7_50
- Guilinger, J. J., Gray, A. B., Barth, N. C., & Fong, B. T. (2020). The Evolution of Sediment Sources Over a Sequence of Postfire Sediment-Laden Flows Revealed Through Repeat High-Resolution Change Detection. *Journal of Geophysical Research: Earth Surface*, 125(10), 1–23. <https://doi.org/10.1029/2020JF005527>
- Harvey, A. M., Mather, A. E., & Stokes, M. (2005). Alluvial fans: Geomorphology, sedimentology, dynamics - Introduction. A review of alluvial-fan research. *Geological Society Special Publication*, 251(1), 1–7. <https://doi.org/10.1144/GSL.SP.2005.251.01.01>
- Jordan, P., Turner, K., Nicol, D., & Boyer, D. (n.d.). *Developing a Risk Analysis Procedure for Post-Wildfire Mass Movement and Flooding in British Columbia*.
- Kean, J. W., & Staley, D. M. (2011). *DIRECT MEASUREMENTS OF THE HYDROLOGIC CONDITIONS LEADING UP TO AND DURING POST-FIRE DEBRIS FLOW IN SOUTHERN CALIFORNIA, USA*. <https://doi.org/10.4408/IJEGE.2011-03.B-075>
- Kean, J. W., Staley, D. M., & Cannon, S. H. (2011). In situ measurements of post-fire debris flows in southern California: Comparisons of the timing and magnitude of 24 debris-flow events with rainfall and soil moisture conditions. *Journal of Geophysical Research: Earth Surface*, 116(4). <https://doi.org/10.1029/2011JF002005>
- Keeley, J. E. (1987). Role of Fire in Seed Germination of Woody Taxa in California Chaparral. *Ecology*, 68(2), 434–443. <https://doi.org/10.2307/1939275>
- Montgomery, D. R., & Dietrich, W. E. (1994). A physically based model for the topographic control on shallow landsliding. In *WATER RESOURCES RESEARCH* (Vol. 30).
- Montgomery, D. R., Schmidt, K. M., Dietrich, W. E., & McKean, J. (2009). Instrumental record

- of debris flow initiation during natural rainfall: Implications for modeling slope stability. *Journal of Geophysical Research*, 114(F1), F01031. <https://doi.org/10.1029/2008JF001078>
- Moody, J. A., Shakesby, R. A., Robichaud, P. R., Cannon, S. H., & Martin, D. A. (2013). Current research issues related to post-wildfire runoff and erosion processes. *Earth Science Reviews*, 122. <https://doi.org/10.1016/j.earscirev.2013.03.004>
- Neary, D. G., Gottfried, G. J., & Ffolliott, P. F. (n.d.). *POST-WILDFIRE WATERSHED FLOOD RESPONSES*.
- Neary, D. G., Koestner, K. A., & Youberg, A. (n.d.). *Hydrologic Impacts of High Severity Wildfire: Learning from the Past and Preparing for the Future*.
- Roy, D. P., Kovalskyy, V., Zhang, H. K., Vermote, E. F., Yan, L., Kumar, S. S., & Egorov, A. (2016). *Characterization of Landsat-7 to Landsat-8 reflective wavelength and normalized difference vegetation index continuity-NC-ND license* (<http://creativecommons.org/licenses/by-nc-nd/4.0/>). <https://doi.org/10.1016/j.rse.2015.12.024>
- Sensing, S. R., Nordal, S., & Lindsay, E. (2017). *Detection of Landslides TBA 4510-Geotechnical Specialization Project Mads Fjeld Abbreviations and Symbols*.
- Staley, D. M., Tillery, A. C., Kean, J. W., Mcguire, L. A., Pauling, H. E., Rengers, F. K., & Smith, J. B. (n.d.). *Estimating post-fire debris-flow hazards prior to wildfire using a statistical analysis of historical distributions of fire severity from remote sensing data*. <https://doi.org/10.1071/WF17122>
- Stolz, A., & Huggel, C. (2008). Debris flows in the Swiss National Park: The influence of different flow models and varying DEM grid size on modeling results. *Landslides*, 5(3), 311–319. <https://doi.org/10.1007/s10346-008-0125-4>
- Swain, D. L., Langenbrunner, B., Neelin, J. D., & Hall, A. (2018). Increasing precipitation volatility in twenty-first-century California. *Nature Climate Change*, 8(5), 427–433. <https://doi.org/10.1038/s41558-018-0140-y>
- Ustin, R. S., & Roberts, D. A. (1996). *MAPPING CHAPARRAL IN THE SANTA MONICA MOUNTAINS USING MULTIPLE ENDMEMBER SPECTRAL " T U R E MODELS*.
- Wisner, B., GeoJournal, H. L.-, & 1993, undefined. (n.d.). Disaster vulnerability: scale, power and daily life. *Springer*. Retrieved from <https://link.springer.com/article/10.1007%252FBF00808129>
- Stolz, A., & Huggel, C. (2008). Debris flows in the Swiss National Park: The influence of different flow models and varying DEM grid size on modeling results. *Landslides*, 5(3), 311–319. <https://doi.org/10.1007/s10346-008-0125-4>
- Billmire, M. E., Elliot, M. J., Endsley, W. J., & Robichaud, K. A. (2015). Rapid response tools and datasets for post-fire modeling: linking Earth Observations and process-based hydrological models to support post-fire remediation. *Remote Sensing & Spatial Information Sciences*, (7), 469–476. <https://doi.org/10.5194/isprsarchives>

- Bisson, M., Favalli, M., Fornaciai, A., Mazzarini, F., Isola, I., Zanchetta, G., & Pareschi, M. T. (n.d.). *A rapid method to assess fire-related debris flow hazard in the Mediterranean region: An example from Sicily (southern Italy)*. <https://doi.org/10.1016/j.jag.2005.04.003>
- Blair, T. C., & Associates, B. (n.d.). *Cause of dominance by sheet-flood vs. debris-flow processes on two adjoining alluvial fans, Death Valley, California*.
- Chen, L., Sela, S., Svoray, T., & Assouline, S. (2013). The role of soil-surface sealing, microtopography, and vegetation patches in rainfall-runoff processes in semiarid areas. *Water Resources Research*, 49(9), 5585–5599. <https://doi.org/10.1002/wrcr.20360>
- Costa, J. E. (1984). Physical geomorphology of debris flows. *Developments and Applications of Geomorphology*, 268–317. https://doi.org/10.1007/978-3-642-69759-3_9
- Cui, Y., Cheng, D., & Chan, D. (2019). Investigation of post-fire debris flows in Montecito. *ISPRS International Journal of Geo-Information*, 8(1). <https://doi.org/10.3390/ijgi8010005>
- Deng, Y., Wu, C., Li, M., & Chen, R. (2015). RND SI: A ratio normalized difference soil index for remote sensing of urban/suburban environments. *International Journal of Applied Earth Observation and Geoinformation*, 39, 40–48. <https://doi.org/10.1016/j.jag.2015.02.010>
- Elkadiri, R., Sultan, M., Youssef, A. M., Chase, R., Bulkhi, A. B., & Al-Katheeri, M. M. (2014). A Remote Sensing-Based Approach for Debris-Flow Susceptibility Assessment Using Artificial Neural Networks and Logistic Regression Modeling. *IEEE JOURNAL OF SELECTED TOPICS IN APPLIED EARTH OBSERVATIONS AND REMOTE SENSING*, 7(12). <https://doi.org/10.1109/JSTARS.2014.2337273>
- Gartner, J. E., Cannon, S. H., Santi, P. M., & Dewolfe, V. G. (2008). Empirical models to predict the volumes of debris flows generated by recently burned basins in the western U.S. *Geomorphology*, 96(3–4), 339–354. <https://doi.org/10.1016/j.geomorph.2007.02.033>
- Goto, E. A., Gray, S., Keller, E., & Clarke, K. C. (2021). *Using Mixed-Methods to Understand Community Vulnerability to Debris Flows in Montecito, CA*. https://doi.org/10.1007/978-3-030-60227-7_50
- Guilinger, J. J., Gray, A. B., Barth, N. C., & Fong, B. T. (2020). The Evolution of Sediment Sources Over a Sequence of Postfire Sediment-Laden Flows Revealed Through Repeat High-Resolution Change Detection. *Journal of Geophysical Research: Earth Surface*, 125(10), 1–23. <https://doi.org/10.1029/2020JF005527>
- Harvey, A. M., Mather, A. E., & Stokes, M. (2005). Alluvial fans: Geomorphology, sedimentology, dynamics - Introduction. A review of alluvial-fan research. *Geological Society Special Publication*, 251(1), 1–7. <https://doi.org/10.1144/GSL.SP.2005.251.01.01>
- Jordan, P., Turner, K., Nicol, D., & Boyer, D. (n.d.). *Developing a Risk Analysis Procedure for Post-Wildfire Mass Movement and Flooding in British Columbia*.
- Kean, J. W., & Staley, D. M. (2011). *DIRECT MEASUREMENTS OF THE HYDROLOGIC CONDITIONS LEADING UP TO AND DURING POST-FIRE DEBRIS FLOW IN SOUTHERN CALIFORNIA, USA*. <https://doi.org/10.4408/IJEGE.2011-03.B-075>
- Kean, J. W., Staley, D. M., & Cannon, S. H. (2011). In situ measurements of post-fire debris

- flows in southern California: Comparisons of the timing and magnitude of 24 debris-flow events with rainfall and soil moisture conditions. *Journal of Geophysical Research: Earth Surface*, 116(4). <https://doi.org/10.1029/2011JF002005>
- Keeley, J. E. (1987). Role of Fire in Seed Germination of Woody Taxa in California Chaparral. *Ecology*, 68(2), 434–443. <https://doi.org/10.2307/1939275>
- Montgomery, D. R., & Dietrich, W. E. (1994). A physically based model for the topographic control on shallow landsliding. In *WATER RESOURCES RESEARCH* (Vol. 30).
- Montgomery, D. R., Schmidt, K. M., Dietrich, W. E., & McKean, J. (2009). Instrumental record of debris flow initiation during natural rainfall: Implications for modeling slope stability. *Journal of Geophysical Research*, 114(F1), F01031. <https://doi.org/10.1029/2008JF001078>
- Moody, J. A., Shakesby, R. A., Robichaud, P. R., Cannon, S. H., & Martin, D. A. (2013). Current research issues related to post-wildfire runoff and erosion processes. *Earth Science Reviews*, 122. <https://doi.org/10.1016/j.earscirev.2013.03.004>
- Neary, D. G., Gottfried, G. J., & Ffolliott, P. F. (n.d.). *POST-WILDFIRE WATERSHED FLOOD RESPONSES*.
- Neary, D. G., Koestner, K. A., & Youberg, A. (n.d.). *Hydrologic Impacts of High Severity Wildfire: Learning from the Past and Preparing for the Future*.
- Roy, D. P., Kovalskyy, V., Zhang, H. K., Vermote, E. F., Yan, L., Kumar, S. S., & Egorov, A. (2016). *Characterization of Landsat-7 to Landsat-8 reflective wavelength and normalized difference vegetation index continuity-NC-ND license* (<http://creativecommons.org/licenses/by-nc-nd/4.0/>). <https://doi.org/10.1016/j.rse.2015.12.024>
- Sensing, S. R., Nordal, S., & Lindsay, E. (2017). *Detection of Landslides TBA 4510-Geotechnical Specialization Project Mads Fjeld Abbreviations and Symbols*.
- Staley, D. M., Tillery, A. C., Kean, J. W., McGuire, L. A., Pauling, H. E., Rengers, F. K., & Smith, J. B. (n.d.). *Estimating post-fire debris-flow hazards prior to wildfire using a statistical analysis of historical distributions of fire severity from remote sensing data*. <https://doi.org/10.1071/WF17122>
- Stolz, A., & Huggel, C. (2008). Debris flows in the Swiss National Park: The influence of different flow models and varying DEM grid size on modeling results. *Landslides*, 5(3), 311–319. <https://doi.org/10.1007/s10346-008-0125-4>
- Swain, D. L., Langenbrunner, B., Neelin, J. D., & Hall, A. (2018). Increasing precipitation volatility in twenty-first-century California. *Nature Climate Change*, 8(5), 427–433. <https://doi.org/10.1038/s41558-018-0140-y>
- Ustin, R. S., & Roberts, D. A. (1996). *MAPPING CHAPARRAL IN THE SANTA MONICA MOUNTAINS USING MULTIPLE ENDMEMBER SPECTRAL " T U R E MODELS*.
- Wisner, B., GeoJournal, H. L., & 1993, undefined. (n.d.). Disaster vulnerability: scale, power and daily life. *Springer*. Retrieved from <https://link.springer.com/article/10.1007%252FBF00808129>

- USGS (2018). Emergency assessment of post-fire debris-flow hazards. Retrieved March 28, 2021, from https://landslides.usgs.gov/hazards/postfire_debrisflow/detail.php?objectid=251
- USGS (2021). Scientific Background. Retrieved March 28, 2021, from https://landslides.usgs.gov/hazards/postfire_debrisflow/background2016.php
- Ustin, R. S., & Roberts, D. A. (1996). *MAPPING CHAPARRAL IN THE SANTA MONICA MOUNTAINS USING MULTIPLE ENDMEMBER SPECTRAL "T U R E MODELS*.
- Watershed Emergency Response Team. (2018, December 14). Woolsey and Hill Fires. Retrieved from <https://www.waterisac.org/system/files/articles/WERT%20Report%20-%20Woolsey%20and%20Hill%20Fires.pdf>
- Weatherbase. (2021). San Gabriel, California Climate Classification. Retrieved April 25, 2021, from [https://www.weatherbase.com/weather/weather-summary.php3?s=587740&cityname=San%2BGabriel%2C%2BCalifornia%2C%2BUnited%2BStates%2Bof%2BAmerica#:~:text=The%20lowest%20recorded%20temperature%20in,17.3%22%20\(439.4%20mm\)](https://www.weatherbase.com/weather/weather-summary.php3?s=587740&cityname=San%2BGabriel%2C%2BCalifornia%2C%2BUnited%2BStates%2Bof%2BAmerica#:~:text=The%20lowest%20recorded%20temperature%20in,17.3%22%20(439.4%20mm)).
- Whiting, D. (2018, October 26). After devastating fires, officials warn winter Rains could bring dangerous debris flows. Retrieved March 28, 2021, from <https://www.ocregister.com/2018/10/26/after-devastating-fires-officials-warn-winter-rains-could-bring-dangerous-debris-flows/>
- Billmire, M. E., Elliot, M. J., Endsley, W. J., & Robichaud, K. A. (2015). Rapid response tools and datasets for post-fire modeling: linking Earth Observations and process-based hydrological models to support post-fire remediation. *Remote Sensing & Spatial Information Sciences*, (7), 469–476. <https://doi.org/10.5194/isprsarchives>
- Bisson, M., Favalli, M., Fornaciai, A., Mazzarini, F., Isola, I., Zanchetta, G., & Pareschi, M. T. (n.d.). *A rapid method to assess fire-related debris flow hazard in the Mediterranean region: An example from Sicily (southern Italy)*. <https://doi.org/10.1016/j.jag.2005.04.003>
- Blair, T. C., & Associates, B. (n.d.). *Cause of dominance by sheet-ood vs. debris-ow processes on two adjoining alluvial fans, Death Valley, California*.
- Chen, L., Sela, S., Svoray, T., & Assouline, S. (2013). The role of soil-surface sealing, microtopography, and vegetation patches in rainfall-runoff processes in semiarid areas. *Water Resources Research*, 49(9), 5585–5599. <https://doi.org/10.1002/wrcr.20360>
- Costa, J. E. (1984). Physical geomorphology of debris flows. *Developments and Applications of Geomorphology*, 268–317. https://doi.org/10.1007/978-3-642-69759-3_9
- Cui, Y., Cheng, D., & Chan, D. (2019). Investigation of post-fire debris flows in Montecito. *ISPRS International Journal of Geo-Information*, 8(1). <https://doi.org/10.3390/ijgi8010005>

- Deng, Y., Wu, C., Li, M., & Chen, R. (2015). RNDISI: A ratio normalized difference soil index for remote sensing of urban/suburban environments. *International Journal of Applied Earth Observation and Geoinformation*, 39, 40–48. <https://doi.org/10.1016/j.jag.2015.02.010>
- Elkadiri, R., Sultan, M., Youssef, A. M., Chase, R., Bulkhi, A. B., & Al-Katheeri, M. M. (2014). A Remote Sensing-Based Approach for Debris-Flow Susceptibility Assessment Using Artificial Neural Networks and Logistic Regression Modeling. *IEEE JOURNAL OF SELECTED TOPICS IN APPLIED EARTH OBSERVATIONS AND REMOTE SENSING*, 7(12). <https://doi.org/10.1109/JSTARS.2014.2337273>
- Gartner, J. E., Cannon, S. H., Santi, P. M., & Dewolfe, V. G. (2008). Empirical models to predict the volumes of debris flows generated by recently burned basins in the western U.S. *Geomorphology*, 96(3–4), 339–354. <https://doi.org/10.1016/j.geomorph.2007.02.033>
- Goto, E. A., Gray, S., Keller, E., & Clarke, K. C. (2021). *Using Mixed-Methods to Understand Community Vulnerability to Debris Flows in Montecito, CA*. https://doi.org/10.1007/978-3-030-60227-7_50
- Guilinger, J. J., Gray, A. B., Barth, N. C., & Fong, B. T. (2020). The Evolution of Sediment Sources Over a Sequence of Postfire Sediment-Laden Flows Revealed Through Repeat High-Resolution Change Detection. *Journal of Geophysical Research: Earth Surface*, 125(10), 1–23. <https://doi.org/10.1029/2020JF005527>
- Harvey, A. M., Mather, A. E., & Stokes, M. (2005). Alluvial fans: Geomorphology, sedimentology, dynamics - Introduction. A review of alluvial-fan research. *Geological Society Special Publication*, 251(1), 1–7. <https://doi.org/10.1144/GSL.SP.2005.251.01.01>
- Jordan, P., Turner, K., Nicol, D., & Boyer, D. (n.d.). *Developing a Risk Analysis Procedure for Post-Wildfire Mass Movement and Flooding in British Columbia*.
- Kean, J. W., & Staley, D. M. (2011). *DIRECT MEASUREMENTS OF THE HYDROLOGIC CONDITIONS LEADING UP TO AND DURING POST-FIRE DEBRIS FLOW IN SOUTHERN CALIFORNIA, USA*. <https://doi.org/10.4408/IJEGE.2011-03.B-075>
- Kean, J. W., Staley, D. M., & Cannon, S. H. (2011). In situ measurements of post-fire debris flows in southern California: Comparisons of the timing and magnitude of 24 debris-flow events with rainfall and soil moisture conditions. *Journal of Geophysical Research: Earth Surface*, 116(4). <https://doi.org/10.1029/2011JF002005>
- Keeley, J. E. (1987). Role of Fire in Seed Germination of Woody Taxa in California Chaparral. *Ecology*, 68(2), 434–443. <https://doi.org/10.2307/1939275>
- Montgomery, D. R., & Dietrich, W. E. (1994). A physically based model for the topographic control on shallow landsliding. In *WATER RESOURCES RESEARCH* (Vol. 30).
- Montgomery, D. R., Schmidt, K. M., Dietrich, W. E., & McKean, J. (2009). Instrumental record of debris flow initiation during natural rainfall: Implications for modeling slope stability. *Journal of Geophysical Research*, 114(F1), F01031. <https://doi.org/10.1029/2008JF001078>
- Moody, J. A., Shakesby, R. A., Robichaud, P. R., Cannon, S. H., & Martin, D. A. (2013). Current research issues related to post-wildfire runoff and erosion processes. *Earth Science Reviews*, 122. <https://doi.org/10.1016/j.earscirev.2013.03.004>

- Neary, D. G., Gottfried, G. J., & Ffolliott, P. F. (n.d.). *POST-WILDFIRE WATERSHED FLOOD RESPONSES*.
- Neary, D. G., Koestner, K. A., & Youberg, A. (n.d.). *Hydrologic Impacts of High Severity Wildfire: Learning from the Past and Preparing for the Future*.
- Roy, D. P., Kovalskyy, V., Zhang, H. K., Vermote, E. F., Yan, L., Kumar, S. S., & Egorov, A. (2016). *Characterization of Landsat-7 to Landsat-8 reflective wavelength and normalized difference vegetation index continuity-NC-ND license* (<http://creativecommons.org/licenses/by-nc-nd/4.0/>). <https://doi.org/10.1016/j.rse.2015.12.024>
- Sensing, S. R., Nordal, S., & Lindsay, E. (2017). *Detection of Landslides TBA 4510-Geotechnical Specialization Project Mads Fjeld Abbreviations and Symbols*.
- Staley, D. M., Tillery, A. C., Kean, J. W., McGuire, L. A., Pauling, H. E., Rengers, F. K., & Smith, J. B. (n.d.). *Estimating post-fire debris-flow hazards prior to wildfire using a statistical analysis of historical distributions of fire severity from remote sensing data*. <https://doi.org/10.1071/WF17122>
- Stolz, A., & Huggel, C. (2008). Debris flows in the Swiss National Park: The influence of different flow models and varying DEM grid size on modeling results. *Landslides*, 5(3), 311–319. <https://doi.org/10.1007/s10346-008-0125-4>
- Swain, D. L., Langenbrunner, B., Neelin, J. D., & Hall, A. (2018). Increasing precipitation volatility in twenty-first-century California. *Nature Climate Change*, 8(5), 427–433. <https://doi.org/10.1038/s41558-018-0140-y>
- Ustin, R. S., & Roberts, D. A. (1996). *MAPPING CHAPARRAL IN THE SANTA MONICA MOUNTAINS USING MULTIPLE ENDMEMBER SPECTRAL " T U R E MODELS*.
- Wisner, B., GeoJournal, H. L., & 1993, undefined. (n.d.). Disaster vulnerability: scale, power and daily life. *Springer*. Retrieved from <https://link.springer.com/article/10.1007%252FBF00808129>

Appendix I. Metadata for Downloaded Files

Satellite Images:

1) Thomas Fire

- Pre-Burn Image:

ID: L1C_T11SKU_A012794_20171203T184735
Acquisition Date: 2017/12/03
Platform: SENTINEL-2A
Tile Number: T11SKU

- Pre-Debris Flow Image:

ID: L1C_T11SKU_A004386_20180107T184933
Acquisition Date: 2018/01/07
Platform: SENTINEL-2B
Tile Number: T11SKU

- Post-Debris Flow Image:

ID: L1C_T11SKU_A013366_20180112T184725
Acquisition Date: 2018/01/12
Platform: SENTINEL-2A
Tile Number: T11SKU

2) Holy Fire

- Pre-Burn Image:

ID: L1C_T11SMT_A007346_20180802T184411
Acquisition Date: 02/08/2018
Platform: SENTINEL-2B
Tile Number: T11SMT
Downloaded: 9/30/2020

- Pre-Debris Flow Image:

ID: LC08_L1TP_040037_20181128_20181211_01_T1
Acquisition Date: 11/28/2018
Platform: Landsat 8
Path: 40
Row: 37
Downloaded: 9/30/2020

- Post-Debris Flow Image:

ID: L1C_T11SMT_A009348_20181220T184200

Acquisition Date: 2018/12/20
Platform: SENTINEL-2B
Tile Number: T11SMT
Downloaded: 9/30/2020

3) Woolsey Fire

- Pre-Burn Image:

ID: L1C_T11SLT_A017613_20181105T183750
Acquisition Date: 2018/11/05
Platform: SENTINEL-2A
Tile Number: T11SLT

- Pre-Debris Flow Image:

ID: L1C_T11SLT_A017899_20181125T184144
Acquisition Date: 2018/11/25
Platform: SENTINEL-2A
Tile Number: T11SLT

- Post-Debris Flow Image:

ID: L1C_T11SLT_A009491_20181230T183754
Acquisition Date: 2018/12/30
Platform: SENTINEL-2B
Tile Number: T11SLT

4) Old and Grand Prix Fires

- Pre-Burn Image:

ID: LT05_L1TP_040036_20031002_20160915_01_T1
Acquisition Date: 2003-10-02
Platform: Landsat 5 TM
Path: 40
Row: 36

- Pre-Debris Flow Image:

ID: LT05_L1TP_040036_20031119_20160914_01_T1
Acquisition Date: 2003-11-19
Platform: Landsat 5 TM
Path: 40
Row: 36

- Post-Debris Flow Image:

ID: LT05_L1TP_040036_20040122_20160914_01_T1
Acquisition Date: 2004-01-22

Platform: Landsat 5 TM
Path: 40
Row: 36

5) Station Fire

- Pre-Burn Image:

ID: LT05_L1TP_041036_20090806_20160907_01_T1
Acquisition Date: 2009-08-06
Platform: Landsat 5 TM
Path: 41
Row: 36

- Pre-Debris Flow Image:

ID: LT05_L1TP_041036_20091110_20160903_01_T1
Acquisition Date: 2009-11-10
Platform: Landsat 5 TM
Path: 41
Row: 36

- Post-Debris Flow Image:

ID: LT05_L1TP_041036_20091126_20160903_01_T1
Acquisition Date: 2009-11-26
Platform: Landsat 5 TM
Path: 41
Row: 36

Digital Elevation Models

I will be using 1/3 arc-second DEMs that are available from the USGS. The cell size for each of these 1-band rasters is approximately 9.5m.

1) Thomas Fire

USGS 13 arc-second n35w119 1 x 1 degree
Published Date: 2019-09-19
Metadata Updated: 2020-03-03
Format: GeoTIFF (437.06 MB), **Extent:** 1 x 1 degree
Downloaded: 2020-09-22

USGS 13 arc-second n35w120 1 x 1 degree
Published Date: 2019-09-24
Metadata Updated: 2020-03-03
Format: GeoTIFF (330.64 MB), **Extent:** 1 x 1 degree
Downloaded: 2020-09-22

2) Holy Fire

USGS 13 arc-second n34w118 1 x 1 degree
Published Date: 2019-09-17
Metadata Updated: 2020-03-03
Format: GeoTIFF (337.45 MB), **Extent:** 1 x 1 degree
Downloaded: 2020-09-30

3) Woolsey Fire

USGS 13 arc-second n35w119 1 x 1 degree
Published Date: 2019-09-19
Metadata Updated: 2020-03-03
Format: GeoTIFF (437.06 MB), **Extent:** 1 x 1 degree
Downloaded: 2020-09-22

4) Station Fire

USGS 13 arc-second n35w119 1 x 1 degree
Published Date: 2019-09-19
Metadata Updated: 2020-03-03
Format: GeoTIFF (437.06 MB), **Extent:** 1 x 1 degree
Downloaded: 2020-09-22

USGS 13 arc-second n35w118 1 x 1 degree
Published Date: 2019-09-24
Metadata Updated: 2020-03-03
Format: GeoTIFF (400.39 MB), **Extent:** 1 x 1 degree
Downloaded: 2020-09-30

Appendix II. Python Codes

1. Mean Index Value

The following is a sample code used to calculate mean dNBR for each watershed. Codes for calculating the other index values are the same, except for input field names and pathnames.

```
Mean_BSI.py

## Name: Erica Byerley
## Date: November 13, 2020
## Purpose: This script calculates the average Bare Soil Index (BSI) of each watershed, adds a field to the watershed feature class,
## and updates the average BSI value of each watershed into this new field.

import arcpy      #Imports Python site package ArcPy
from arcpy import env    #Imports environment class from ArcPy
env.workspace = "C:/Users/ebyer/Documents/NAU/Thesis/ThesisPro/Holy_Fire.gdb" #Sets the default workspace
env.overwriteoutput = True #Enables overwriting of files

- if arcpy.CheckExtension("spatial") == "Available": #If the spatial analyst license is available
    arcpy.CheckOutExtension("spatial") #Checks out the spatial analyst license
    from arcpy.sa import * #Imports all functions of the spatial analyst extension
    BSIraster = arcpy.Raster("Holy_preDF_BSI_Clip1_Proj") #Uses a variable to hold a raster object
    watersheds = "Holy_Watersheds" #Uses variable to hold feature class
    newfield = "PreDF_BSI" #Uses variable to hold a new field name for BSI values
    fieldname = arcpy.ValidateFieldName(newfield) #Calls a function to validate the new field name
    fieldlist = arcpy.ListFields(watersheds) #Calls the ListFields function to create a list of field objects
    fieldnames = [] #Creates a blank list
    for field in fieldlist: #Iterates over each element in fieldlist
        fieldnames.append(field.name) #Append an element to fieldnames
    if fieldname not in fieldnames: #Starts an if structure
        arcpy.AddField_management(watersheds, newfield, "FLOAT") #Adds new field if not present
        print "New field has been added." #Prints that the new field has been added
    else: #If the field already exists
        print "Field name already exists." #Lets user know, does not add new field

    #Creates an Update Cursor for geometry & Mean_BSI field in watersheds
    with arcpy.da.UpdateCursor(watersheds, ["SHAPE@", "PreDF_BSI"]) as cursor:
        for row in cursor: #Iterates through each row in the table
            outmask = arcpy.sa.ExtractByMask(BSIraster, row[0]) #Uses watershed geometry to create BSI raster
            mean = outmask.mean #Uses variable to hold mean BSI value in watershed
            row[1] = mean #Sets the Mean_BSI field to the mean value
            print mean #Prints value to interactive window to show progress
            cursor.updateRow(row) #Updates the row with the mean BSI value
            del outmask, mean #Deletes variables to be used in next iteration
        del row, cursor #Releases database lock when all rows have been updated

    arcpy.CheckInExtension("spatial") #Checks spatial analyst license back in
- else: #If the spatial analyst license is not available
    print "Spatial Analyst license is not available." #Prints message saying it's unavailable

#Prints message to let user know the task is complete
print "Congratulations, mean BSI values for each watershed have been updated in the PreDF_BSI field!"
```


2. Mean K Factor

```
Mean_KF_RF.py

## Name: Erica Byerley
## Date: March 4, 2021
## Purpose: This script adds a 'Mean_KF_RF' field to the watershed attribute table, calculates the average rock-free K factor value for soil up
## to 20cm deep for each watershed, and updates the value in the attribute table. This tool works with a KFactor_RockFree raster generated from
## the gNATSGO database.

import arcpy #Imports Python site package ArcPy
from arcpy import env #Imports environment class from ArcPy
env.workspace = "C:/Users/ebyer/Documents/NAU/Thesis/ThesisPro/GrandPrix_Old_Fires.gdb" #Sets the default workspace
env.overwriteoutput = True #Enables overwriting of files

-if arcpy.CheckExtension("spatial") == "Available": #If the spatial analyst license is available
    arcpy.CheckOutExtension("spatial") #Checks out the spatial analyst license
    from arcpy.sa import * #Imports all functions of the spatial analyst extension

    watersheds = "OldGrandPrix_Watersheds" #Uses variable to hold feature class
    KF_RF = arcpy.Raster("OGP_KF_RockFree") #Uses variable to hold raster object
    #Uses variable to hold reclassification values to be used with the Reclassify tool
    remap = arcpy.sa.RemapValue([['',0],['.02',2],['.05',5],['.10',10],['.15',15],['.17',17],['.20',20],['.24',24],['.28',28],['.32',32],['.37',37],\
    ['.43',43],['.49',49],['.55',55]])
    Reclass_KF_RF = arcpy.sa.Reclassify(KF_RF, "KFACTRF_DC", remap, "NODATA") #Reclassifies the KF_RF raster

    newfield = "Mean_KF_RF" #Uses variable to hold a new field name for dNBR values
    fieldname = arcpy.ValidateFieldName(newfield) #Calls a function to validate the new field name
    fieldlist = arcpy.ListFields(watersheds) #Calls the ListFields function to create a list of field objects
    fieldnames = [] #Creates a blank list
    for field in fieldlist: #Iterates over each element in fieldlist
        fieldnames.append(field.name) #Append an element to fieldnames
    if fieldname not in fieldnames: #Starts an if structure
        arcpy.AddField_management(watersheds, newfield, "FLOAT") #Adds new field if not present
        print "New field has been added." #Prints that the new field has been added
    else: #If the field already exists
        print "Field name already exists." #Lets user know, does not add new field

    #Creates an Update Cursor for geometry & Mean_KF_RF field in watersheds
    with arcpy.da.UpdateCursor(watersheds, ["SHAPE@", "Mean_KF_RF"]) as cursor: #Creates an update cursor
        for row in cursor: #Iterates through each row in the table
            outmask = arcpy.sa.ExtractByMask(Reclass_KF_RF, row[0]) #Uses watershed geometry to create KF raster
            mean = outmask.mean #Uses variable to hold mean KF value in watershed
            row[1] = mean/100 #Sets the Mean_KF_RF field to the mean value
            print mean/100 #Prints value to interactive window to show progress
            cursor.updateRow(row) #Updates the row with the mean KF value
            del outmask, mean #Deletes variables to be used in next iteration
            del row, cursor #Releases database lock when all rows have been updated

    arcpy.CheckInExtension("spatial") #Checks spatial analyst license back in
-else: #If the spatial analyst license is not available
    print "Spatial Analyst license is not available." #Prints message saying it's unavailable

#Prints message to let user know the task is complete
print "Congratulations, mean KF_RF values for each watershed have been updated in the Mean_KF_RF field!"
```

3. Percent Clay

```
PercentClay.py

## Name: Erica Byerley
## Date: March 4, 2021
## Purpose: This script adds a 'PercClay' field to the watershed attribute table, calculates the average clay content for soil up to 20cm deep
## for each watershed, and updates the value in the attribute table. This tool works with a Percent Clay raster from the gNATSGO database that
## has been reclassified to 10x the percent clay value.

import arcpy    #Imports Python site package ArcPy
from arcpy import env    #Imports environment class from ArcPy
env.workspace = "C:/Users/ebyer/Documents/NAU/Thesis/ThesisPro/Thomas_Fire.gdb" #Sets the default workspace

-if arcpy.CheckExtension("spatial") == "Available": #If the spatial analyst license is available
    arcpy.CheckOutExtension("spatial") #Checks out the spatial analyst license
    from arcpy.sa import * #Imports all capabilities from the spatial analyst extension
    env.overwriteOutput = True #Enables overwriting of files

    watersheds = "Thomas_Watersheds" #Uses variable to hold feature class
    PercentClay = arcpy.Raster("Thomas_PercClay_Reclass") #Uses variable to hold raster object for percent clay

    newfield = "PercClay" #Uses variable to hold a new field name for percent clay values
    fieldname = arcpy.ValidateFieldName(newfield) #Calls a function to validate the new field name
    fieldlist = arcpy.ListFields(watersheds) #Calls the ListFields function to create a list of field objects
    fieldnames = [] #Creates a blank list
    - for field in fieldlist: #Iterates over each element in fieldlist
        fieldnames.append(field.name) #Append an element to fieldnames
    - if fieldname not in fieldnames: #Starts an if structure
        arcpy.AddField_management(watersheds, newfield, "FLOAT") #Adds new field if not present
        print "New field has been added." #Prints that the new field has been added
    - else: #If the field already exists
        print "PercClay field already exists." #Lets user know, does not add new field

    #Creates an Update Cursor for geometry & PercClay field in watersheds
    - with arcpy.da.UpdateCursor(watersheds, ["SHAPE@", "PercClay"]) as cursor:
        - for row in cursor: #Iterates through each row in the table
            outmask = arcpy.sa.ExtractByMask(PercentClay, row[0]) #Uses watershed geometry to create percent clay raster
            mean = outmask.mean #Uses variable to hold mean percent clay value in watershed
            - if outmask.mean is None: #If there is no outmask mean value
                row[1] = None #Sets the value in the watersheds attribute table to Null
            - else: #If there is a mean value for the outmask
                row[1] = (mean/10) #Sets the PercClay field to the mean value
                print (mean/10) #Prints value to interactive window to show progress
                cursor.updateRow(row) #Updates the row with the mean KF value
                del outmask, mean #Deletes variables to be used in next iteration
            del row, cursor #Releases database lock when all rows have been updated

    arcpy.CheckInExtension("spatial") #Checks spatial analyst license back in
    - else: #If the spatial analyst license is not available
        print "Spatial Analyst license is not available." #Prints message saying it's unavailable

    #Prints message to let user know the task is complete
    print "Congratulations, mean PercClay values for each watershed have been updated in the PercClay field!"
```

4. Hypsometric Integral

```
HypsometricIntegral.py

## Name: Erica Byerley
## Date: October 12, 2020
## Purpose: This script calculates the hypsometric integral of each watershed and adds a field
## to the watershed feature class containing this value. This is based on the Pike and Wilson (1971)
## method of estimating HI.

import arcpy    #Imports Python site package ArcPy
from arcpy import env    #Imports environment class from ArcPy
env.workspace = "C:/Users/ebyer/Documents/NAU/Thesis/ThesisPro/Thomas_Fire.gdb" #Sets the default workspace
env.overwriteoutput = True #Enables overwriting of files

-if arcpy.CheckExtension("spatial") == "Available": #If the spatial analyst license is available
    arcpy.CheckOutExtension("spatial") #Checks out the spatial analyst license
    from arcpy.sa import * #Imports all functions of the spatial analyst extension
    DEM = arcpy.Raster("Thomas_DEM") #Uses a variable to hold a raster object
    watersheds = "Thomas_WS_2" #Uses variable to hold feature class
    newfield = "HI" #Uses variable to hold a new field name for hypsometric integral
    fieldname = arcpy.ValidateFieldName(newfield) #Calls a function to validate the new field name
    fieldlist = arcpy.ListFields(watersheds) #Calls the ListFields function to create a list of field objects
    fieldnames = [] #Creates a blank list
    for field in fieldlist: #Iterates over each element in fieldlist
        fieldnames.append(field.name) #Append an element to fieldnames
    - if fieldname not in fieldnames: #Starts an if structure
        arcpy.AddField_management(watersheds, newfield, "FLOAT") #Adds new field if not present
        print "New field has been added." #Prints that the new field has been added
    - else: #If the field already exists
        print "Field name already exists." #Lets user know, does not add new field

    #Creates an Update Cursor for geometry & HI field in watersheds
    with arcpy.da.UpdateCursor(watersheds, ["SHAPE@", "HI"]) as cursor:
        for row in cursor: #Iterates through each row in the table
            outmask = arcpy.sa.ExtractByMask(DEM, row[0]) #Uses watershed geometry to create DEM
            Have = outmask.mean #Uses variable to hold mean DEM value in watershed
            Hmax = outmask.maximum #Uses variable to hold maximum DEM value
            Hmin = outmask.minimum #Uses variable to hold minimum DEM value
            HI = (Have - Hmin) / (Hmax - Hmin) #Calculates hypsometric integral, stores in a variable
            row[1] = HI #Sets the HI field to the HI value
            print HI #Prints value to interactive window to show progress
            cursor.updateRow(row) #Updates the row with the HI value
            del outmask, Have, Hmax, Hmin, HI #Deletes variables to be used in next iteration
        del row, cursor #Releases database lock when all rows have been updated

    arcpy.CheckInExtension("spatial") #Checks spatial analyst license back in
-else: #If the spatial analyst license is not available
    print "Spatial Analyst license is not available." #Prints message saying it's unavailable

#Prints message to let user know the task is complete
-print "Congratulations, hypsometric integral values have been updated in the HI field!"
```

5. Slope and Burn Severity (dNBR)

```
Slope23_SevBurn.py

## Name: Erica Byerley
## Date: October 23, 2020
## Purpose: This script calculates the proportion of each watershed burned at high or moderate severity
## and with gradients in excess of 23 degrees. It creates a field in the watershed feature class and
## writes calculated values for each watershed into this field.

import arcpy #Imports Python site package ArcPy
from arcpy import env #Imports environment class from ArcPy
env.workspace = "C:/Users/ebyer/Documents/NAU/Thesis/ThesisPro/GrandPrix_Old_Fires.gdb" #Sets the default workspace
env.overwriteoutput = True #Enables overwriting of files

if arcpy.CheckExtension("spatial") == "Available": #If the spatial analyst license is available
    arcpy.CheckOutExtension("spatial") #Checks out the spatial analyst license
    from arcpy.sa import * #Imports all functions of the spatial analyst extension
    Slope = arcpy.Raster("OldGrandPrix_Slope") #Uses variable to hold raster object
    dNBR = arcpy.Raster("OGP_dNBR_Clip") #Uses variable to hold raster object
    watersheds = "OldGrandPrix_Watersheds" #Uses variable to hold feature class
    newfield = "SevBurnSlope" #Uses variable to hold a new field name
    fieldname = arcpy.ValidateFieldName(newfield) #Calls a function to validate the new field name
    fieldlist = arcpy.ListFields(watersheds) #Calls the ListFields function to create a list of field objects
    fieldnames = [] #Creates a blank list
    for field in fieldlist: #Iterates over each element in fieldlist
        fieldnames.append(field.name) #Append an element to fieldnames
    if fieldname not in fieldnames: #Starts an if structure
        arcpy.AddField_management(watersheds, newfield, "FLOAT") #Adds new field if not present
        print "New field has been added." #Prints that the new field has been added
    else: #If the field already exists
        print "Field name already exists." #Lets user know, does not add new field

#Creates an Update Cursor for geometry & Slope23_SevBurn field in watersheds
with arcpy.da.UpdateCursor(watersheds, ["SHAPE@", "SHAPE@AREA", "SevBurnSlope"]) as cursor:
    for row in cursor: #Iterates through each row in the table
        outmask1 = arcpy.sa.ExtractByMask(Slope, row[0]) #Uses watershed geometry to create Slope raster
        WS_Slope = outmask1 > 23 #Creates Boolean raster for slopes greater than 23 degrees
        outmask2 = arcpy.sa.ExtractByMask(dNBR, row[0]) #Uses watershed geometry to create dNBR raster
        WS_dNBR = outmask2 >= 0.27 #Creates Boolean raster for moderate or high-severity burned areas
        WS1 = outmask1 > 0.0000 #Reclassifies slope outmask so entire watershed has a value of 1
        finalraster = WS_Slope * WS_dNBR #Multiplies Boolean rasters together
        WS_area = row[1] #Sets variable to the SHAPE@AREA token value for each watershed

        #Gets the cell size in the x dimension from the finalraster
        GetCellSizeX = arcpy.GetRasterProperties_management(finalraster, "CELLSIZEX")
        CellSizeX = GetCellSizeX.getOutput(0) #Stores x cell size in variable
        print CellSizeX #Prints value to interactive window
        #Gets the cell size in the y dimension from the finalraster
        GetCellSizeY = arcpy.GetRasterProperties_management(finalraster, "CELLSIZEY")
        CellSizeY = GetCellSizeY.getOutput(0) #Stores y cell size in variable
        print CellSizeY #Prints value to interactive window
        #Converts finalraster to a numpy array
        numpy_array1 = arcpy.RasterToNumPyArray(finalraster)
        #Counts all cells with value of 1 in the finalraster
        count_valuel = float(numpy.count_nonzero(numpy_array1 == 1))
        print count_valuel #Prints value to interactive window
        #Calculates the finalraster area as the cell size in each dimension multiplied by the count_valuel
        finalraster_area = count_valuel * float(CellSizeX) * float(CellSizeY)
        Slope23_SevBurn = finalraster_area / WS_area #Calculates Slope23_SevBurn value

        row[2] = Slope23_SevBurn #Sets the Slope23_SevBurn field to the Slope23_SevBurn value
        print Slope23_SevBurn #Prints value to interactive window to show progress
        cursor.updateRow(row) #Updates the row with the Slope23_SevBurn value
        del outmask1, outmask2, WS_Slope, WS_dNBR, WS1, finalraster, Slope23_SevBurn #Deletes variables
        del row, cursor #Releases database lock when all rows have been updated

    arcpy.CheckInExtension("spatial") #Checks spatial analyst license back in
else: #If the spatial analyst license is not available
    print "Spatial Analyst license is not available." #Prints message saying it's unavailable

#Prints message to let user know the task is complete
print "Congratulations, values have been calculated for the proportion of each watershed \
burned at high or moderate severity and with slopes in excess of 23 degrees. These values \
have been updated in the Slope23_SevBurn field!"
```


6. Slope and Burn Severity (BAER)

```
BAER_23.py

## Name: Erica Byerley
## Date: October 23, 2020
## Purpose: This script determines the proportion of each watershed with high slope and burned at moderate or high severity
## according to BAER classification values. It updates these values into the BAER_23 field in the watershed attribute table.
## Please note: All inputs must use the same units for cell size.

import arcpy #Imports Python site package ArcPy
from arcpy import env #Imports environment class from ArcPy
env.workspace = "C:/Users/ebyer/Documents/NAU/Thesis/ThesisPro/Holy_Fire.gdb" #Sets the default workspace
env.overwriteoutput = True #Enables overwriting of files

if arcpy.CheckExtension("spatial") == "Available": #If the spatial analyst license is available
    arcpy.CheckOutExtension("spatial") #Checks out the spatial analyst license
    from arcpy.sa import * #Imports all functions of the spatial analyst extension
    Slope = arcpy.Raster("Holy_Slope") #Uses variable to hold raster object
    BAER = arcpy.Raster("Holy_BAER_BurnSev") #Uses variable to hold raster object
    watersheds = "Holy_Watersheds" #Uses variable to hold feature class
    newfield = "BAER_23" #Uses variable to hold a new field name
    fieldname = arcpy.ValidateFieldName(newfield) #Calls a function to validate the new field name
    fieldlist = arcpy.ListFields(watersheds) #Calls the ListFields function to create a list of field objects
    fieldnames = [] #Creates a blank list
    for field in fieldlist: #Iterates over each element in fieldlist
        fieldnames.append(field.name) #Append an element to fieldnames
    if fieldname not in fieldnames: #Starts an if structure
        arcpy.AddField_management(watersheds, newfield, "FLOAT") #Adds new field if not present
        print "New field has been added." #Prints that the new field has been added
    else: #If the field already exists
        print "Field name already exists." #Lets user know, does not add new field

    #Creates an Update Cursor for geometry & BAER_23 field in watersheds
    with arcpy.da.UpdateCursor(watersheds, ["SHAPE@", "SHAPE@AREA", "BAER_23"]) as cursor:
        for row in cursor: #Iterates through each row in the table
            outmask1 = arcpy.sa.ExtractByMask(Slope, row[0]) #Uses watershed geometry to create Slope raster
            WS_Slope = outmask1 > 23 #Creates Boolean raster for slopes greater than 23 degrees
            outmask2 = arcpy.sa.ExtractByMask(BAER, row[0]) #Uses watershed geometry to create BAER raster
            remap = RemapRange([[0,2,0],[3,4,1],[5,255,0]]) #Uses variable to hold values for reclassification
            #Reclassifies BAER outmask to Boolean raster, hold result in variable
            WS_BAER = arcpy.sa.Reclassify(outmask2, "VALUE", remap, "NODATA")
            finalraster = WS_Slope * WS_BAER #Multiplies Boolean rasters together
            WS1 = outmask1 > 0.0000 #Reclassifies slope outmask so entire watershed has a value of 1
            WS_area = row[1] #Sets variable to the SHAPE@AREA token value for each watershed

            #Gets the cell size in the x dimension from the finalraster
            GetCellSizeX = arcpy.GetRasterProperties_management(finalraster, "CELLSIZEX")
            CellSizeX = GetCellSizeX.getOutput(0) #Stores x cell size in variable
            print CellSizeX #Prints value to interactive window
            #Gets the cell size in the y dimension from the finalraster
            GetCellSizeY = arcpy.GetRasterProperties_management(finalraster, "CELLSIZEY")
            CellSizeY = GetCellSizeY.getOutput(0) #Stores y cell size in variable
            print CellSizeY #Prints value to interactive window
            #Converts finalraster to a numpy array
            numpy_array1 = arcpy.RasterToNumPyArray(finalraster)
            #Counts all cells with value of 1 in the finalraster
            count_value1 = float(numpy.count_nonzero(numpy_array1 == 1))
            print count_value1 #Prints value to interactive window
            #Calculates the finalraster area as the cell size in each dimension multiplied by the count_value1
            finalraster_area = count_value1 * float(CellSizeX) * float(CellSizeY)

            BAER_23 = finalraster_area / WS_area #Calculates the BAER_23 value
            row[2] = BAER_23 #Sets the BAER_23 field to the BAER_23 value
            print BAER_23 #Prints value to interactive window to show progress
            cursor.updateRow(row) #Updates the row with the BAER_23 value
            del outmask1, outmask2, WS_Slope, WS_BAER, WS1, finalraster, BAER_23 #Deletes variables
        del row, cursor #Releases database lock when all rows have been updated

    arcpy.CheckInExtension("spatial") #Checks spatial analyst license back in
else: #If the spatial analyst license is not available
    print "Spatial Analyst license is not available." #Prints message saying it's unavailable

#Prints message to let user know the task is complete
print "Congratulations, values have been calculated for the proportion of each watershed \
burned at high or moderate severity and with slopes in excess of 23 degrees. These values \
have been updated in the BAER_23 field!"
```

Appendix III. Ordinary Least Squares Regression Tables

1. Thomas Fire

Summary of OLS Results - Model Variables

Variable	Coefficient [a]	StdError	t-Statistic	Probability [b]	Robust_SE	Robust_t	Robust_Pr [b]	VIF [c]
Intercept	0.487940	0.242293	2.013838	0.045925*	0.210309	2.320105	0.021761*	-----
MEAN_DNBR	-1.685386	0.321541	-5.241585	0.000001*	0.274654	-6.136403	0.000000*	2.734577
PREDF_NDSI	-2.049346	0.530316	-3.864384	0.000176*	0.473121	-4.331552	0.000031*	1.089258
BAER_23	1.248586	0.217183	5.749004	0.000000*	0.174551	7.153149	0.000000*	2.463880
MEAN_KF_WS	1.663849	0.445577	3.734141	0.000281*	0.375468	4.431400	0.000021*	1.422920

2. Holy Fire

Summary of OLS Results - Model Variables

Variable	Coefficient [a]	StdError	t-Statistic	Probability [b]	Robust_SE	Robust_t	Robust_Pr [b]	VIF [c]
Intercept	-2.567937	2.180976	-1.177425	0.269252	1.456916	-1.762584	0.111801	-----
MEAN_DNBR	4.096065	3.198531	1.280608	0.232380	2.556996	1.601905	0.143654	14.785697
PREDF_NDSI	18.808599	7.269349	2.587384	0.029318*	4.369683	4.304340	0.002005*	1.740917
BAER_23	-2.089391	2.011549	-1.038697	0.326060	1.609021	-1.298548	0.226416	16.985706
MEAN_KF_WS	-4.582596	2.413457	-1.898769	0.090047	1.396633	-3.281174	0.009537*	1.440482
PERCCLAY	0.045132	0.106667	0.423113	0.682131	0.086519	0.521646	0.614483	1.402517

3. Woolsey Fire

Summary of OLS Results - Model Variables

Variable	Coefficient [a]	StdError	t-Statistic	Probability [b]	Robust_SE	Robust_t	Robust_Pr [b]	VIF [c]
Intercept	-3.496539	1.398549	-2.500119	0.019990*	1.058841	-3.302232	0.003114*	-----
SEVBURNSLOPE	1.856159	0.657740	2.822026	0.009669*	0.677573	2.739423	0.011684*	2.441225
PREDF_BSI	5.400516	2.229800	2.421973	0.023725*	1.779167	3.035418	0.005881*	6.802576
PREDF_NDSI	-7.399736	2.867062	-2.580948	0.016708*	2.093471	-3.534674	0.001771*	13.928507
PREDF_NDVI	6.171414	2.724875	2.264843	0.033255*	1.719853	3.588337	0.001553*	4.861185
MEAN_KF_WS	4.405895	2.523935	1.745645	0.094217	2.116521	2.081668	0.048689*	3.386364
PERCCLAY	0.071378	0.026577	2.685757	0.013200*	0.021665	3.294709	0.003171*	4.971807

4. Station Fire

Summary of OLS Results - Model Variables

Variable	Coefficient [a]	StdError	t-Statistic	Probability [b]	Robust_SE	Robust_t	Robust_Pr [b]	VIF [c]
Intercept	-0.720775	0.559098	-1.289176	0.238451	0.336973	-2.138973	0.069616	-----
MEAN_DNBR	-1.310844	0.813887	-1.610597	0.151381	0.367754	-3.564464	0.009236*	1.127970
MEAN_NDSI	10.617980	2.679618	3.962498	0.005569*	1.633830	6.498828	0.000309*	1.746376
SEVBURNSLOPE	1.858290	0.325806	5.703678	0.000780*	0.220423	8.430562	0.000011*	1.742211
MEAN_KF_WS	-1.569453	0.964298	-1.627560	0.147714	0.446740	-3.513120	0.009880*	2.186393

ProQuest Number: 28491717

INFORMATION TO ALL USERS

The quality and completeness of this reproduction is dependent on the quality and completeness of the copy made available to ProQuest.



Distributed by ProQuest LLC (2021).

Copyright of the Dissertation is held by the Author unless otherwise noted.

This work may be used in accordance with the terms of the Creative Commons license or other rights statement, as indicated in the copyright statement or in the metadata associated with this work. Unless otherwise specified in the copyright statement or the metadata, all rights are reserved by the copyright holder.

This work is protected against unauthorized copying under Title 17,
United States Code and other applicable copyright laws.

Microform Edition where available © ProQuest LLC. No reproduction or digitization of the Microform Edition is authorized without permission of ProQuest LLC.

ProQuest LLC
789 East Eisenhower Parkway
P.O. Box 1346
Ann Arbor, MI 48106 - 1346 USA